

Portland State University

PDXScholar

Dissertations and Theses

Dissertations and Theses

8-1-1969

Physical and kinetic properties of dihydroorotate dehydrogenase from *Lactobacillus bulgaricus*

Craig David Taylor
Portland State University

Follow this and additional works at: https://pdxscholar.library.pdx.edu/open_access_etds

Let us know how access to this document benefits you.

Recommended Citation

Taylor, Craig David, "Physical and kinetic properties of dihydroorotate dehydrogenase from *Lactobacillus bulgaricus*" (1969). *Dissertations and Theses*. Paper 62.

<https://doi.org/10.15760/etd.62>

This Thesis is brought to you for free and open access. It has been accepted for inclusion in Dissertations and Theses by an authorized administrator of PDXScholar. Please contact us if we can make this document more accessible: pdxscholar@pdx.edu.

AN ABSTRACT OF THE THESIS OF Craig David Taylor for the Master of Science in Biology presented August 29, 1969.

Title: Physical and Kinetic Properties of Dihydroorotate Dehydrogenase from Lactobacillus bulgaricus.

APPROVED BY MEMBERS OF THE THESIS COMMITTEE:

[REDACTED]
Herman Taylor, Chairman

[REDACTED]
Earl Fisher, Jr.

[REDACTED]
John W. Myers

[REDACTED]
David McClure

Dihydroorotate (DHO) dehydrogenase catalyzes the oxidation of DHO to orotate in the pyrimidine biosynthetic pathway. This enzyme was originally isolated from a bacterium, Zymobacterium oroticum, which would ferment orotate as a sole source of energy. This adaptive catabolic enzyme, which catalyzes the reduction of orotate to DHO in an efficient pyridine nucleotide-linked reaction, has been extensively studied by several workers. Until recently, no study has been carried out on the enzyme which catalyzes the reaction in the biosynthetic direction. Preliminary studies have shown that the biosynthetic enzyme in Esherichia

coli and a pseudomonad is not capable of reducing orotate to DHO by a pyridine nucleotide-linked reaction. These results suggested that there may be significant differences between the catabolic and biosynthetic enzymes.

In the present study biosynthetic DHO dehydrogenase from Lactobacillus bulgaricus was investigated on the basis of physical and kinetic properties in order to compare the enzyme with the extensively studied catabolic enzyme. The stoichiometry exhibited by the DHO oxidase activity of the biosynthetic enzyme and the absorption spectrum suggest that biosynthetic DHO dehydrogenase is a flavoprotein. Thin layer chromatography of the flavins extracted from the enzyme and reactivation of apoenzymes specific for flavin mononucleotide or flavin adenine dinucleotide have shown that the enzyme contains flavin mononucleotide.

The demonstration of enzyme-catalyzed sulfite autoxidation suggested that iron is present and is involved in electron transport. Inhibitor studies have shown that the enzyme contains sulfhydryl groups and the inactivation of such groups halts internal electron transport early in the sequence.

Kinetic studies were carried out including the determination of the K_m for dihydroorotate, K_i for orotate, and the pH optimum. The kinetic behavior of the enzyme in the presence of various inhibitors suggest that the essential sulfhydryl groups reside at or near the active site.

Ammonium sulfate was found to enhance the activity of the enzyme. Evidence presented suggested that this phenomenon is probably an unspecific anion effect in which the rate constant for the breakdown of the enzyme substrate complex is directly affected.

A possible scheme of the internal electron transport of biosynthetic DHO dehydrogenase was presented, using the data from this thesis and additional evidence from studies carried out by other workers on similar enzymes. A summary of the physical and kinetic properties of biosynthetic and catabolic DHO dehydrogenase was presented and a detailed comparison between the two enzymes made.

PHYSICAL AND KINETIC PROPERTIES OF DIHYDROOROTATE
DEHYDROGENASE FROM LACTOBACILLUS BULGARICUS

by

Craig David Taylor

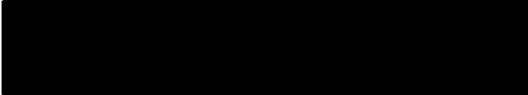
A thesis submitted in partial fulfillment of the
requirements for the degree of

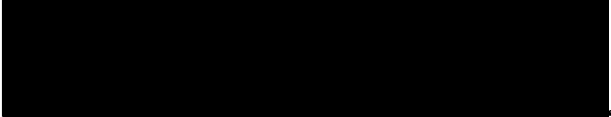
MASTER OF SCIENCE
in
BIOLOGY

Portland State University
1969


TO THE OFFICE OF GRADUATE STUDIES:

The members of the Committee approve the thesis of
Craig David Taylor presented August 29, 1969.

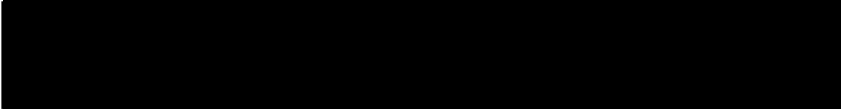

Herman Taylor, Chairman

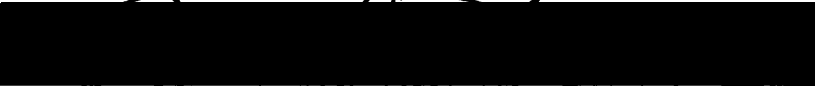

Earl Fisher, Jr.


John W. Myers


David McClure

APPROVED:


Earl Fisher, Jr., Head, Department of Biology


Frank L. Roberts, Acting Dean of Graduate Studies

August 29, 1969

TABLE OF CONTENTS

	PAGE
LIST OF TABLES.	vi
LIST OF FIGURES	vii
INTRODUCTION.	1
MATERIALS AND METHODS	5
Organism.	5
Growth and Harvest of the Organism.	5
Preparation of Cell Free Extracts	7
Purification of Enzymes	7
DHO Dehydrogenase	7
NADPH Cytochrome c Reductase.	9
D-amino Acid Oxidase.	9
Enzyme Assays and Chemical Determinations	9
Ferricyanide Assay.	9
2,6-Dichlorophenolindophenol and Cytochrome c Reduction Assays.	10
Aerobic Assay	10
Converting Optical Density Change into Micromolar Changes.	10
Inhibitor Studies	10
Sulfite Autoxidation.	10
Assay of NADPH Cytochrome c Reductase	11
Assay of D-amino Acid Oxidase	11

Measurement of the Rate of Oxygen Consumption, Orotate Formation, and Hydrogen Peroxide Production.	11
Flavin Analysis Using Thin Layer Chromatography.	13
Flavin Analysis Using apo-NADPH Cytochrome c Reductase and apo-D-Amino Acid Oxidase.	14
Commercial Sources of Chemicals and Enzymes.	14
RESULTS.	16
Evidence for DHO Dehydrogenase Being a Flavoprotein.	16
Aerobic Production of Hydrogen Peroxide.	16
Visible Spectrum of Dihydroorotate Dehydrogenase	17
Qualitative Analysis for Flavin.	17
Effect of pH	22
Determination of K_m for DHO and K_i for Orotate	29
Effect of Ammonium Sulfate	32
Effect of Sulfhydryl Inhibitors.	36
Indirect Evidence that Iron is Involved in Catalysis	48
Evidence Relating to the Flow of Electrons in Biosynthetic DHO Dehydrogenase	50
Reduction of Various Electron Acceptors by Dihydroorotate Dehydrogenase	55
DISCUSSION	57
Internal Electron Transport.	57
Catabolic DHO Dehydrogenase.	57
Xanthine Oxidase	58
Biosynthetic DHO Dehydrogenase	59
Comparison of Catabolic and Biosynthetic DHO Dehydrogenase	61

	PAGE
SUMMARY	64
REFERENCES	65
APPENDIX	68

LIST OF TABLES

TABLE	PAGE
I Growth Medium for <u>Lactobacillus Bulgaricus</u>	6
II Thin Layer Chromatography of the Flavins Extracted from Biosynthetic Dihydroorotate Dehydrogenase	23
III Effect of the Flavins from Biosynthetic Dihydroorotate Dehydrogenase on Reactivation of apo-NADPH-Cyto- chrome c Reductase and apo-Amino Acid Oxidase. . . .	24
IV Effect of Salts on Biosynthetic Dihydroorotate Dehydro- genase Activity.	35
V Reversal of Sulfhydryl Inhibition by Mercaptoethanol	49
VI Effect of Tiron and p-Hydroxymercuribenzoate on Dihydro- orotate Dehydrogenase Activity with Various Electron Acceptors.	54
VII Rate of Oxidation of Dihydroorotate to Orotate by Bio- synthetic Dihydroorotate Dehydrogenase using Various Electron Acceptors	56
VIII Properties of Catabolic and Biosynthetic Dihydroorotate Dehydrogenase.	62

LIST OF FIGURES

FIGURE		PAGE
1	Pyrimidine biosynthetic pathway in microorganisms.	2
2	The stoichiometry expected if dihydroorotate dehydro- genase is a flavoprotein	16
3	Comparison of the oxygen uptake and hydrogen peroxide production during conversion of dihydroorotate to orotate by biosynthetic dihydroorotate dehydro- genase	18
4	Absorption spectrum of biosynthetic dihydroorotate dehydrogenase.	20
5	The effect of pH on biosynthetic dihydroorotate dehydro- genase activity.	25
6	The effect of orotate concentration on biosynthetic dihydroorotate dehydrogenase activity.	27
7	The effect of orotate concentration on K_m for dihydro- orotate.	30
8	The effect of ammonium sulfate on biosynthetic dihydro- orotate dehydrogenase activity	33
9	The effect of ammonium sulfate on the pH optimum of biosynthetic dihydroorotate dehydrogenase.	37
10	Effect of ammonium sulfate on the K_m for dihydroorotate. . .	39

11	The effect of mercuric chloride on biosynthetic dihydroorotate dehydrogenase activity and protection by dihydroorotate.	41
12	The effect of p-hydroxymercuribenzoate on biosynthetic dihydroorotate dehydrogenase activity and protection by dihydroorotate	43
13	Protection of biosynthetic dihydroorotate dehydrogenase from mercuric chloride inhibition by orotate	46
14	Initiation of sulfite autoxidation by biosynthetic dihydroorotate dehydrogenase	51
15	Internal electron transport in catabolic dihydroorotate dehydrogenase.	57
16	Internal electron transport in xanthine oxidase.	58
17	Proposed sequence of internal electron transport in biosynthetic dihydroorotic dehydrogenase	59

INTRODUCTION

Biosynthetic dihydroorotate dehydrogenase (DHO dehydrogenase) catalyzes the oxidation of dihydroorotate (DHO) to orotate in the pyrimidine biosynthetic pathway. In studies carried out by Lieberman and Kornberg for the establishment of the pathway of orotate breakdown, catabolic DHO dehydrogenase was first isolated from Zymobacterium oroticum, an organism capable of fermenting orotic acid. From conclusions attained in this and subsequent studies, by these and other workers, (1,2,3,4) the sequence of pyrimidine biosynthesis occurs as shown in Figure 1.

Beginning with the work of Lieberman and Kornberg (5) a series of detailed studies were carried out on the induced catabolic DHO dehydrogenase. It was found that the enzyme catalyzes the reduction of orotate by NADH (5), the oxidation of NADH by oxygen as well as the oxidation of DHO by NAD^+ and oxygen (6).

Analysis on purified extracts (6) and crystalline enzyme (7,8,9) revealed that the enzyme was a non-heme iron, labile sulfhydryl containing flavoprotein, unique in the fact that the prosthetic groups, flavin adenine dinucleotide (FAD) and flavin mononucleotide (FMN) were present in a molar ratio of one. Detailed equilibrium (10), kinetic (6,7,8,9) electron paramagnetic resonance spectroscopy (8,11,12,13,14,15,16) studies, as well as investigations of subunit structure (17) have been carried out on catabolic DHO dehydrogenase.

Throughout the period of study it has generally been presumed,

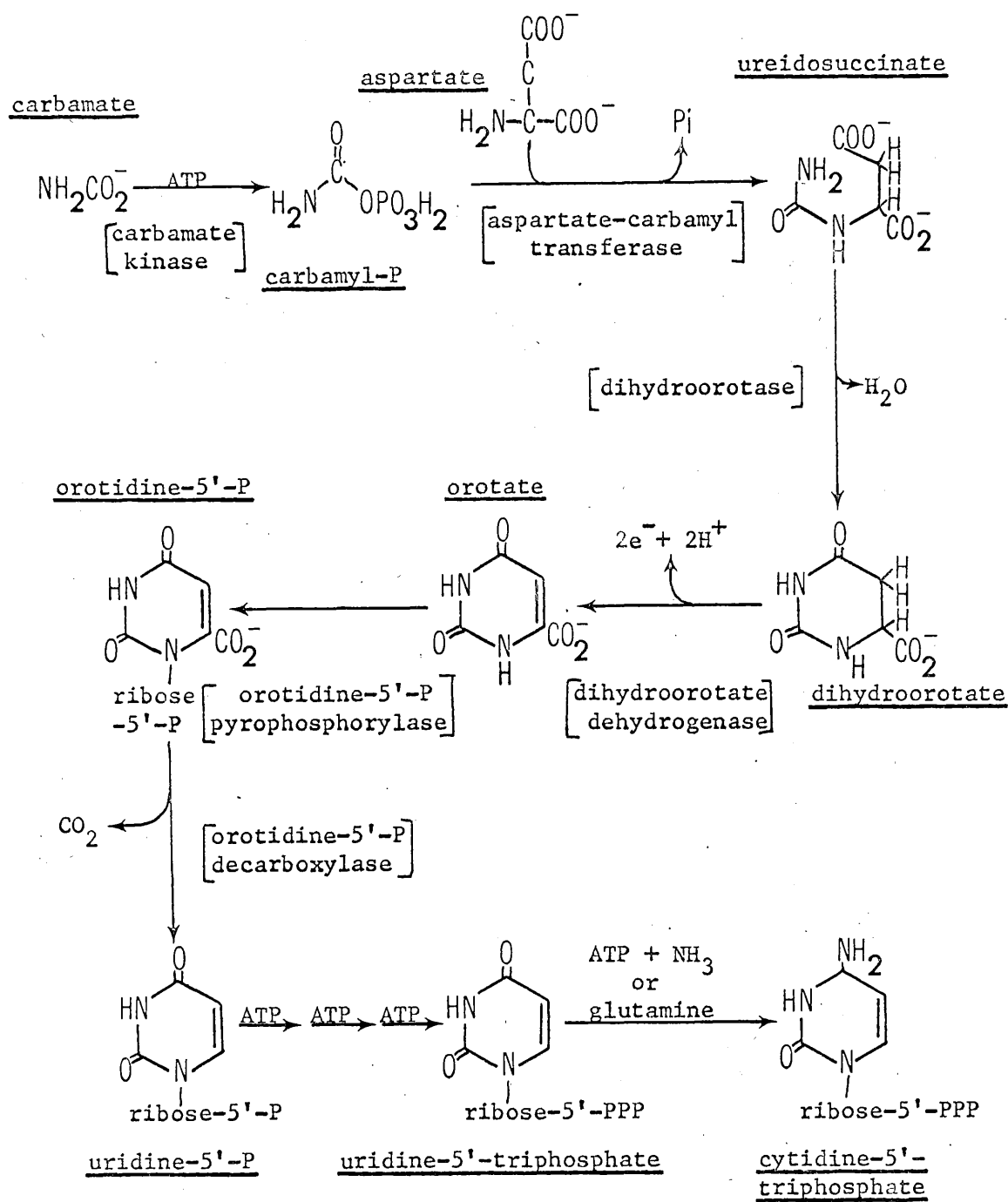


Figure 1. Pyrimidine biosynthetic pathway in microorganisms

with acceptance (4, p.726), that catabolic and biosynthetic DHO dehydrogenase are the same protein molecule. Workers have recognized that catabolic DHO dehydrogenase is an adaptive enzyme (6,18) and have noted that the oxidation of DHO may not be pyridine nucleotide linked (6). It has recently been stated that the more efficient reduction of orotate by NADH is not of physiological consequence in light of the biosynthetic reaction (16). However no attempt was made to isolate biosynthetic DHO dehydrogenase for comparative purposes.

Utilizing the findings of Yates and Pardee (19,20) that the pyrimidine pathway in E. coli was repressible, the laboratory of Taylor and Taylor partially purified biosynthetic DHO dehydrogenase from derepressed pyrimidine mutants of E. coli (21). They found that the particle bound E. coli biosynthetic enzyme differed from the Z. oroticum enzyme in that it was not linked to NADH neither as an electron donor for the reduction of orotate nor as a NADH oxidase. Further data supporting this finding were obtained in the same laboratory from a soil pseudomonad (22). This organism, which was capable of utilizing orotate as a sole or supplemental energy and carbon source, produced a constitutive, particle bound, synthetic DHO dehydrogenase as well as synthesizing a soluble catabolic enzyme in response to the introduction of orotate. After separation of the two activities by centrifugation, studies revealed that the induced, catabolic enzyme demonstrated activities similar to those of the Z. oroticum enzyme, while the biosynthetic enzyme had catalytic properties similar to that isolated from E. coli. This general observation was later supported by other work (23,24). A soluble biosynthetic enzyme was found to be present in the anaerobic

organism Lactobacillus bulgaricus. This organism requires a pyrimidine precursor for growth (25) and was found to produce comparatively large amounts of biosynthetic DHO dehydrogenase upon derepression by starvation for pyrimidine (26). The DHO dehydrogenase has been extensively purified from extracts of derepressed cells in this laboratory.

The object of this study was to determine the general physical and kinetic properties of biosynthetic DHO dehydrogenase from L. bulgaricus so that a comparison could be made with the catabolic enzyme isolated from Z. oroticum.

MATERIALS AND METHODS

Organism

Lactobacillus bulgaricus 09, ATCC 13866. This organism requires a pyrimidine for growth. Ureidosuccinate, dihydroorotate, orotate, or uracil satisfy this requirement.

Growth and Harvest of the Organism (26)

Cultures were maintained by transfer every three days into liquid medium. The medium, a modification of that of Wright et al. (27), is described in Table I.

The medium was sterilized by autoclaving and inoculated soon after cooling. If the sterile medium had been stored it was steamed and cooled before inoculation to regain nearly anaerobic conditions. Cultures were incubated at 37°.

The cells were released from repression as follows: 100 ml of an exponentially growing culture was transferred to 500 ml of fresh medium and incubated overnight. The resulting culture was then diluted into two liters of fresh medium, incubated 8 to 10 hours, and then forced into derepression by transferring the 2.6 liters into 10 liters of fresh medium containing no orotate. The culture was allowed to incubate until the pH of the growth medium had reached pH 4.5 to 4.3 (12 to 16 hours). The cells were then harvested by continuous flow centrifugation at 0° in a Servall refrigerated centrifuge. The resulting cell pellets were washed twice with 0.05 M Tris-HCl buffer (pH 7.6) containing 1 mM magnesium chloride.

TABLE I
GROWTH MEDIUM FOR LACTOBACILLUS BULGARICUS

<u>Material</u>	<u>Amount</u> g/liter
Vitamin-free casamino acids	5.0
Casitone	10.0
K ₂ HPO ₄	0.5
KH ₂ PO ₄	0.5
Glucose	20.0
Sodium acetate · 3H ₂ O	10.0
MgSO ₄ · 7H ₂ O	0.2
NaCl	0.01
MnSO ₄ · 4H ₂ O	0.01
Trisodium citrate	0.25
	mg/liter
Adenine	5.0
Guanine	5.0
Xanthine	3.0
Pyridoxal · HCl	0.25
Thiamine	1.0
Calcium pantothenate	1.0
Riboflavin	1.0
Niacin	1.0
p-Aminobenzoic acid	0.5
Pyridoxine	2.0
Folic acid	0.25
	µg/liter
Biotin	5.0
Vitamin B-12	2.0
Tween-80	1.0 ml

Preparation of Cell Free Extracts (26)

L. bulgaricus extract was prepared by resuspending the cells (0.3 g/ml) in 0.05 M Tris-HCl buffer (pH 7.6) containing 1 mM magnesium chloride and passing through a French Pressure Cell (American Instrument Co.) at 7,000 psi. The extract was supplemented with sodium orotate to a final concentration of 0.6 mM and centrifuged at 150,000 X g for 90 minutes at 0° in a Beckman model L refrigerated ultracentrifuge (Ti-50 head). The pellets were discarded and the clear yellow supernatant was used as the starting material for the purification of DHO dehydrogenase.

Purification of Enzymes (26)

DHO Dehydrogenase. All of the following steps were carried out at 0° :

1. 0.025 volume of 1 M manganese chloride was added dropwise to the 150,000 X g supernatant, with stirring. The stirring was allowed to continue for 15 minutes after the last portion of the manganese chloride was added. The extract was frozen at this point until further purification was undertaken.

2. The manganese treated extract was thawed and a sufficient amount of 0.2 M EDTA (pH 7.0) was added to give a final concentration of 0.01 M. The pH of the extract was then lowered to 4.1 by the addition of 0.5 M sodium acetate buffer (pH 3.8) with stirring. The precipitated nucleic acid was removed by centrifugation at 10,000 X g for 10 minutes and the clear yellow extract passed through a Sephadex G-25 column equilibrated with AOV buffer [0.01 M sodium acetate buffer (pH 5.65) containing 0.6 mM sodium orotate, and 1 mM EDTA]. This process was used

to exchange buffer systems and to remove the free flavins and low molecular weight compounds contained in the extract.

3. The enzymatically active fractions from the G-25 column were combined and solid sodium chloride was added to give a final concentration of 0.15 M. Utilizing a batch procedure the enzyme was adsorbed to Sephadex DEAE cellulose equilibrated with AOV containing 0.15 M sodium chloride. The DEAE was washed once each with AOV containing 0.15 M sodium chloride and AOV containing 0.20 M sodium chloride (wash volume was about one third the combined volume of the G-25 extract). The enzyme was then eluted with a minimum amount of AOV containing 0.40 M sodium chloride.

4. The enzyme fractions from the DEAE cellulose were pooled and an equal volume of saturated ammonium sulfate (at 0°) was added with stirring. Then solid ammonium sulfate was quickly added until the extract reached 80% saturation. Protein began to precipitate at 60% saturation. As soon as the solid ammonium sulfate dissolved the precipitate containing the enzyme was recovered by centrifugation. The pellets were well drained, and redissolved in a minimum amount of AOV.

5. The enzyme fraction was clarified by centrifugation and quickly applied to a 1.5 X 84 cm Sephadex G-200 column equilibrated with AOV. Fractions were collected at a rate of 5 ml/hour.

6. The most active Sephadex G-200 fractions were pooled and further purified by polyacrylamide preparative disc electrophoresis with a Polyprep apparatus (Buchler Instruments, Fort Lee, N.J.) cooled by circulating fluid from an external bath adjusted to -1°. The general procedure, preparation of the gels and Tris buffer systems were carried out

as stated by Jovin et al. (28). For enzyme stability 0.6 mM sodium orotate was included in all reagents and buffers. The samples were run through 2.0 cm of a 7% resolving gel at an applied current of 40 ma. The sample was eluted at a rate of 24 ml/hr and collected in a refrigerated fraction collector. For enzyme stability the fractions were adjusted to pH 5.6 with 0.5 M sodium acetate buffer (pH 3.8). The most active fractions constitute a 230 fold purification over derepressed cells (23,000 fold over repressed cells) with a specific activity of about 6000 units/mg of protein (protein concentration was difficult to determine accurately at this concentration). Unless otherwise stated all studies were carried out on the enzyme at this state of purity.

NADPH Cytochrome c Reductase. NADPH cytochrome c reductase from brewer's yeast was purified through the ethanol precipitation step and resolved for FMN by the method of Hass et al. (29).

D-amino Acid Oxidase. D-amino acid oxidase from an acetone powder of pig kidney (30) was purified and resolved for FAD by the method of Huennekens and Felton (31).

Enzyme Assays and Chemical Determinations

Ferricyanide Assay. DHO dehydrogenase activity was measured by a modified form of the ferricyanide reduction assay of Taylor and Taylor (21). The assay mixture (3 ml) contained 300 μ moles of Tris-HCl buffer (pH 7.6 to 7.8), 36 μ moles of sodium dihydroorotate, 2.0 μ moles of potassium ferricyanide, and 1.0 to 6.0 units of enzyme. The reaction was initiated by adding DHO and potassium ferricyanide (0.5 ml total) to the other components. The reduction of ferricyanide was followed spectrophotometrically with a Coleman Hitachi 124 double beam spectrophotometer

at 420 nm or colorimetrically with a Klett-Summerson colorimeter equipped with a #42 filter.

2,6-Dichlorophenolindophenol and Cytochrome c Reduction Assays.

2,6-Dichlorophenolindophenol (DCI, 0.2 umoles) and cytochrome c (1.0 mg) replaced potassium ferricyanide in assays using these compounds as the electron acceptor. The reduction of the acceptors were followed spectrophotometrically at 600 nm for DCI and 550 nm for cytochrome c.

Aerobic Assay. DHO dehydrogenase activity was also measured by an aerobic assay similar to that of Yates and Pardee (19) where oxygen was used as the electron acceptor. The increase in the concentration of orotate was followed spectrophotometrically at 282 nm.

Converting Optical Density Change into Micromolar Changes. Standard curves were prepared for each instrument and conversion factors were calculated to relate change in optical density to umoles of DHO oxidized or orotate produced.

One unit of enzyme is that amount which will oxidize 1 μ mole of DHO (or produce 1 μ mole of OA) per hour.

Inhibitor Studies. Inhibition studies were carried out using a modified form of the standard ferricyanide assay. A given amount of inhibitor was incubated with the buffer, enzyme, water portion of the standard assay system (volume 2.5 ml) for a determined length of time and the reaction initiated by adding DHO and potassium ferricyanide (0.5 ml total). The reaction was followed spectrophotometrically and the initial reaction rates recorded.

Sulfite Autoxidation. Sulfite autoxidation was measured manometrically (9) in a Gilson differential respirometer by conventional

techniques (32). Oxygen uptake was followed in a reaction mixture (2 ml) consisting of 200 μ moles of potassium phosphate buffer (pH 7.6), 2 μ moles EDTA, 24 μ moles sodium dihydroorotate, 100 μ moles sodium sulfite, and about 6 units of DHO dehydrogenase. Mannitol (300 μ moles) or Tiron (0.5 or 1.0 μ moles) were also added to some flasks. The reaction was initiated by tipping in enzyme and sodium sulfite from separate side arms.

Assay of NADPH Cytochrome c Reductase. NADPH cytochrome c reductase was assayed spectrophotometrically as described by Huennekens and Felton (31).

Assay of D-amino Acid Oxidase. D-amino acid oxidase was assayed manometrically in a Gilson differential respirometer by the procedure of Huennekens and Felton (31).

Measurement of the Rate of Oxygen Consumption, Orotate Formation, and Hydrogen Peroxide Production. The reaction mixture (4ml) contained 400 μ moles of Tris-HCl buffer (pH 7.6), 48 μ moles of sodium dihydroorotate, 300 units of DHO dehydrogenase (0.13 ml of a 2390 unit/ml of solution, specific activity 5,270 units/mg of protein), and 20 μ g of catalase (when indicated). All components except DHO and catalase, which were added to separate sidearms, were dispensed into the main well of a respirometer flask. The reaction was initiated by tipping in the DHO and allowed to proceed with shaking at 23°.

Oxygen consumption was measured manometrically with a Gilson differential respirometer (32).

The production of hydrogen peroxide was measured by a modification of the chromogen reaction commonly used in blood glucose analysis

(33,34,35) involving a peroxidase catalized oxidation of o-dianisidine dihydrochloride (3,3-dimethoxybenzidine dihydrochloride) by hydrogen peroxide. The chromogen mixture (50 ml) contained 7.89 μ moles (2.5 mg) of o-dianisidine dihydrochloride, 40 μ g of peroxidase, and 6 mmoles of sodium phosphate buffer (pH 7.0). The o-dianisidine solution was stored as a 5 mg/ml aqueous stock and the peroxidase as a stock containing 1 mg in 25 ml of 0.12 M sodium phosphate buffer (pH 7.0). These stocks were stable at 4° for a few weeks. At the desired time intervals a sample (0.2 ml) was withdrawn from the respirometer flask specified for the hydrogen peroxide determination and diluted into 5.8 ml of the chromogen mixture. The mixture was allowed to react for 10 minutes and the intensity of the color measured spectrophotometrically at 455 nm in a Bausch and Lomb 505 spectrophotometer. The blank was prepared by adding 0.20 ml of an enzyme reaction mixture without DHO in place of the sample. A commercial solution of 30% hydrogen peroxide was standardized by the manometric measurement of the oxygen evolved upon the addition of catalase. Dilutions of freshly standardized solutions were used in the preparation of a standard curve for the o-dianisidine assay. A calculated amount of DHO dehydrogenase was added to the chromogen mixture used for the standard curves to more closely approximate the conditions of the assay.

Orotate production was measured by withdrawing samples (0.2 ml) at various times from a designated respirometer flask, diluting into 2.8 ml of 5% trichloroacetic acid (TCA), and measuring the absorbance due to orotate at 284 nm (DHO does not absorb significantly at this wave length). The protein concentration was not great enough to exhibit any

precipitation. The blank was prepared by diluting 0.20 ml of an enzyme solution containing no DHO into 2.8 ml of 5% TCA. A standard curve was prepared with known concentrations of orotate added to DHO-free, enzyme-containing reaction mixtures.

Flavin Analysis Using Thin Layer Chromatography. Extraction of flavins from the enzyme (specific activity about 3,000 units/mg of protein) was carried out at room temperature by a method similar to that of Kondo et al. (36), the flavins being protected from light to minimize photolytic reactions. The enzyme, pooled from Buchler electrophoresis runs, were heated in a boiling water bath for 2 minutes, and the denatured protein removed by centrifugation. The flavins were separated from the solution by quickly extracting with 0.4 volume of water-saturated phenol.¹ The phenol layer was separated from the extracted aqueous layer and the flavins returned to a small amount of fresh water (0.1 to 0.2 ml) by shaking the mixture with two volumes of diethyl ether. The aqueous layer was subjected to a light vacuum to remove the residual ether. During the heating process some of the protein was broken down into ninhydrin detectable amino acids and peptides which were extracted into the phenol. When in sufficient concentration, these contaminants caused streaking of the flavin spots during chromatography. A second rapid extraction with phenol usually separated the flavins away from enough of these compounds to yield satisfactory chromatographic results.²

¹For best results the phenol was surfaced with a 1/8 to 1/4 inch layer of water. Prior to use the two phases were shaken to an emulsion, allowed to separate, and the phenol removed with a Pasteur pipette.

²If a second phenol extraction yields unsatisfactory results it would best be replaced by eluting the contaminants away from the flavins

The aqueous flavin solution was lyophilized to dryness and stored at -20° . The flavins were dissolved in a minimum amount of water and qualitatively identified by thin layer chromatography on cellulose gel MN 300 using the nucleotide solvent system t-amyl alcohol, formic acid, and water (3:2:1 v/v) or on Silica gel G using pyridine, acetic acid and water (10:1:40 v/v) (37).

Flavin Analysis Using apo-NADPH Cytochrome c Reductase and apo-D-Aminoacid Oxidase. After removal from the enzyme by the procedure previously mentioned, the flavins were qualitatively analyzed from aliquots of the boiled extracts (clarified by centrifugation if needed) using the apo-NADPH cytochrome c reductase (specific for FMN) and apo-D-aminoacid oxidase (specific for FAD) assay systems (31).

Commercial Sources of Chemicals and Enzymes

Brinkmann Instrument Co. Cellulose gel MN-300, MN-300 DEAE cellulose.

G. Frederick Smith Chemical Co. Tiron.

Mallinckrodt Chemical Co. Mannitol.

Mann Research Laboratories. 2-mercaptoethanol, orotic acid.

Matheson, Coleman and Bell. Sodium 2,6-dichlorophenolindophenol.

E. Merk, Distributed by Brinkmann Instrument Co. Silica gel G.

Pharmacia Fine Chemicals, Inc. DEAE Sephadex A-50, Sephadex G-25, G-200.

by thin layer ion exchange chromatography on MN DEAE cellulose using 0.05 N hydrochloric acid and then eluting the flavins with 0.1 N hydrochloric acid. The hydrochloric acid is then quickly removed under vacuum.

Sigma Chemical Co. Catalase (1 mg decomposes 3,000 μ moles of hydrogen peroxide/min); cytochrome c, Type III; o-dianisidine dihydrochloride; dihydroorotic acid; ethylenediamine tetraacetate, disodium salt, Sigma grade; flavin adenine dinucleotide, grade III; flavin mononucleotide, commercial grade; p-hydroxymercuribenzoate, sodium salt.

RESULTS

Evidence for DHO Dehydrogenase Being a Flavoprotein

It was found early in the development of a purification scheme for the biosynthetic enzyme from L. bulgaricus that the bright yellow color of the crude extract (150,000 X g supernatant) was due mainly to free flavins rather than flavoproteins. Passage of the yellow manganese-treated extract through Sephadex G-25 resulted in relatively colorless active fractions. This observation left open the question of whether or not the biosynthetic enzyme was a flavoprotein.

Aerobic Production of Hydrogen Peroxide. It is generally accepted (9) that flavoproteins which catalyze oxidase type reactions reduce the oxygen to hydrogen peroxide. Since L. bulgaricus DHO dehydrogenase is capable of catalyzing the oxidation of DHO aerobically, the reaction might be expected to proceed as shown in Figure 2 if it is indeed a flavoprotein.

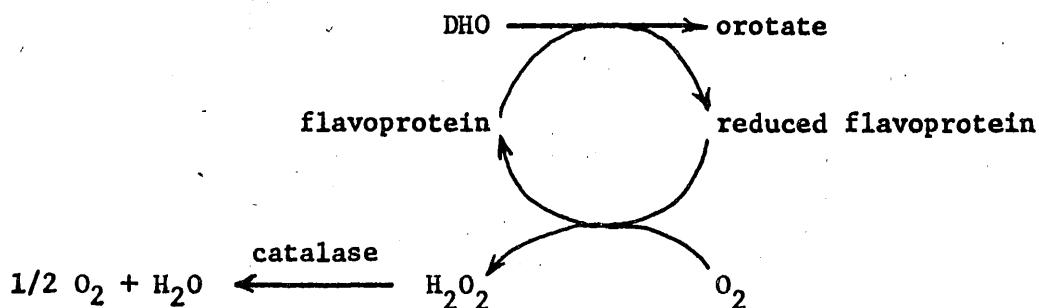


Figure 2. The stoichiometry expected if dihydroorotate dehydrogenase is a flavoprotein.

An experiment was carried out as described in Methods in which the rate

of oxygen consumption, orotate and hydrogen peroxide production were measured. If biosynthetic DHO dehydrogenase is a flavoprotein one would expect the stoichiometry of Figure 2 to be followed, namely the rates of oxygen consumption, orotate and hydrogen peroxide production will be equal. Also, if catalase were added at the beginning of the experiment, the hydrogen peroxide formed would be immediately broken down into oxygen and water as shown in Figure 2. This occurrence would decrease the observed oxygen consumption by one half. The results shown in Figure 3 show that the stoichiometry exhibited by DHO dehydrogenase is typical of a flavoprotein. The hydrogen peroxide was stable in the reaction mixture as shown by the convergence of the curves resulting from catalase added at the beginning and the end of the experimental period.

Visible Spectrum of Dihydroorotate Dehydrogenase. Upon further purification the characteristic yellow color of flavoproteins became evident in concentrated fractions. Figure 4 shows the visible spectrum of the most purified fraction of the enzyme from the preparative disc electrophoresis separation. The spectrum is typical of a flavoprotein with distinct maxima at 380,466 nm and minima at 350,416 nm. There is a noticeable shoulder at about 490 nm similar to those present in other flavoproteins (38,39,40,41,7,8,9,). The ultraviolet absorption peak observed for flavoproteins between 265 and 280 nm is obscured in this preparation due to the presence of orotate which has a maximal absorption at 282 nm.

Qualitative Analysis for Flavin. Qualitative analysis for flavins (see Methods) carried out on pooled preparative disc electrophoresis

Figure 3. Comparison of the oxygen uptake and hydrogen peroxide production during conversion of dihydroorotate to orotate by biosynthetic dihydroorotate dehydrogenase.

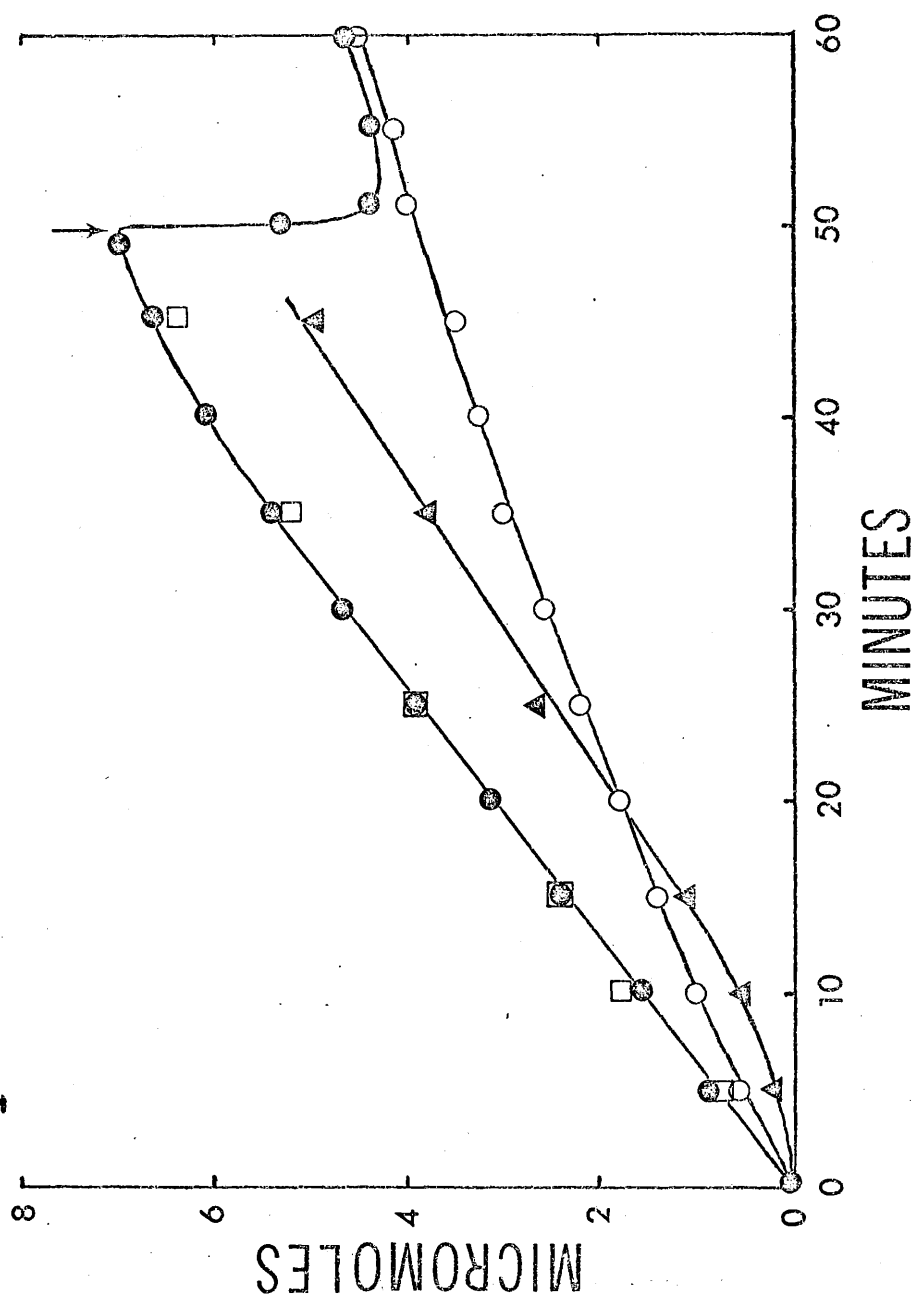


Figure 3. Comparison of the oxygen uptake and hydrogen peroxide production during conversion of dihydroorotate to orotate by biosynthetic dihydroorotate dehydrogenase.

The reaction mixtures and procedures were as stated in Methods. Symbols: (O), total μ moles of oxygen consumed, catalase added at the arrow; (●), total μ moles of oxygen consumed when catalase was present from the beginning of the experiment; (□), total μ moles of orotate produced; (Δ), total μ moles of hydrogen peroxide produced.

Figure 4. Absorption spectrum of biosynthetic dihydroorotate dehydrogenase.

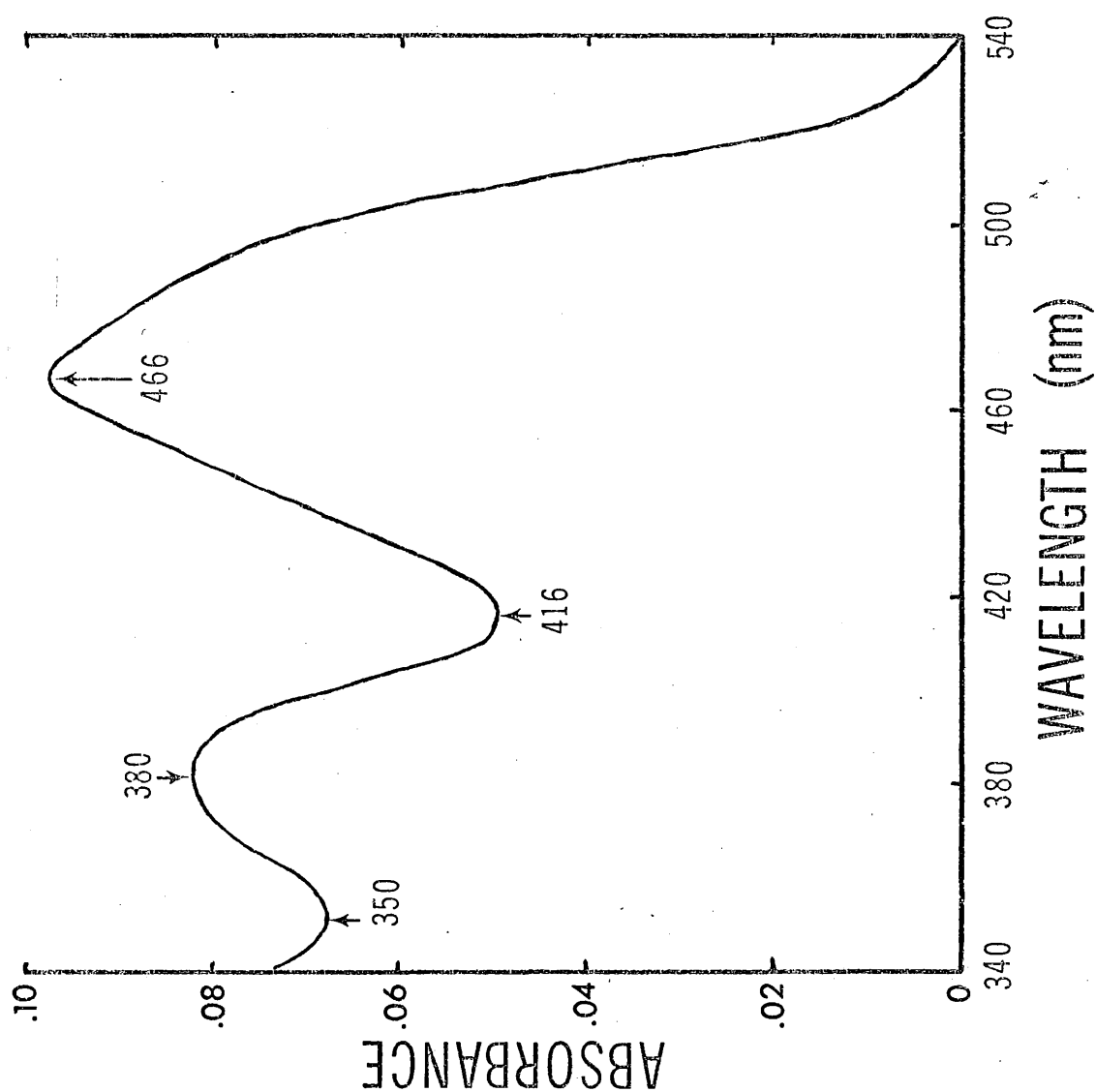


Figure 4. Absorption spectrum of biosynthetic dihydroorotate dehydrogenase.

The spectrum was obtained with the most active fraction of the preparative disk electrophoresis preparation. The sample contained about 0.6 mg of protein/ml and had a specific activity of about 6,000 units/mg of protein. The solution also contained 0.6 mM sodium orotate.

fractions suggest that biosynthetic DHO dehydrogenase contains FMN. Results of the thin layer chromatographic analysis are shown in Table II. In both thin layer systems used flavin obtained from boiled extract migrated as a single spot with an R_f very close to that of FMN standards. The unknown migrated as FMN when mixed with chromatographically purified FAD and as a single spot when mixed with chromatographically purified FMN. Flavin adenine dinucleotide was not noticeably hydrolyzed to FMN when carried through the same heat treatment and extraction procedure as the unknown.

Further supporting evidence is shown in Table III. The flavins in the unknown are capable of reactivating apo-NADPH-cytochrome c reductase but not apo-D-aminoacid oxidase, suggesting that only FMN is present in the biosynthetic enzyme.

Effect of pH

The variation of enzyme activity with pH is shown in Figure 5, representing two experiments performed 10 days apart. The pH optimum most probably lies between 7.6 and 7.8, the determination of which is made somewhat difficult by the fact that there is no large change (about 17%) in the enzyme activity over the entire pH range measured.

It is possible that pH curves such as those in Figure 5 represent a composite effect of pH on K_m (Michaelis constant) as well as on enzyme activity. Sufficient increases in K_m with pH can occur such that the substrate concentration used in the assay is no longer saturating, thus causing a decrease in reaction rate (42). This limitation can be overcome by obtaining enough data at each pH to obtain Lineweaver-Burk plots

TABLE II
THIN LAYER CHROMATOGRAPHY OF THE FLAVINS EXTRACTED
FROM BIOSYNTHETIC DIHYDROOROTATE
DEHYDROGENASE

Sample	t-amyl alcohol-formic acid - water. (Sta- tionary phase, MN 300 cellulose gel)	Pyridine - acetic acid - water. (Sta- tionary phase, silica gel G)
	Rf	Rf
Riboflavin	0.675	----
FMN	0.528	0.524
FAD	0.260	0.720
Unknown	0.526	0.540

The solvents and procedure were as stated in Methods.

TABLE III

EFFECT OF THE FLAVINS FROM BIOSYNTHETIC DIHYDROOROTATE DEHYDROGENASE
ON REACTIVATION OF apo-NADPH-CYTOCHROME c REDUCTASE
AND apo-D-AMINOACID OXIDASE

Concentration of added flavin in reaction mix- ture; ml of unknown added.	Reaction Rate	
	NADPH cytochrome c reductase	D-amino acid oxidase
μM	OD ₅₅₀ /min	$\mu\text{l O}_2$ consumed/min
<u>FMN</u>		
0.0667	0.0365	----
0.0533	0.0270	----
0.0333	0.0230	----
None	0.0165	----
<u>FAD</u>		
0.333	----	8.3
None	----	3.7
<u>Unknown</u>		
0.05 ml (equivalent to about 0.03 μM flavin)	0.0225	----
0.10 ml (equivalent to about 0.06 μM flavin)	0.0280	----
0.60 ml (equivalent to about 0.36 μM flavin)	----	3.6

The preparation of the apoenzymes and the assay procedures were as stated in Methods. The unknown consisted of a heat treated 1/10 dilution in water of a 3,000 unit/ml solution of biosynthetic DHO dehydrogenase (specific activity about 6,000 units/mg of protein).

Figure 5. The effect of pH on biosynthetic dihydroorotate dehydrogenase activity.

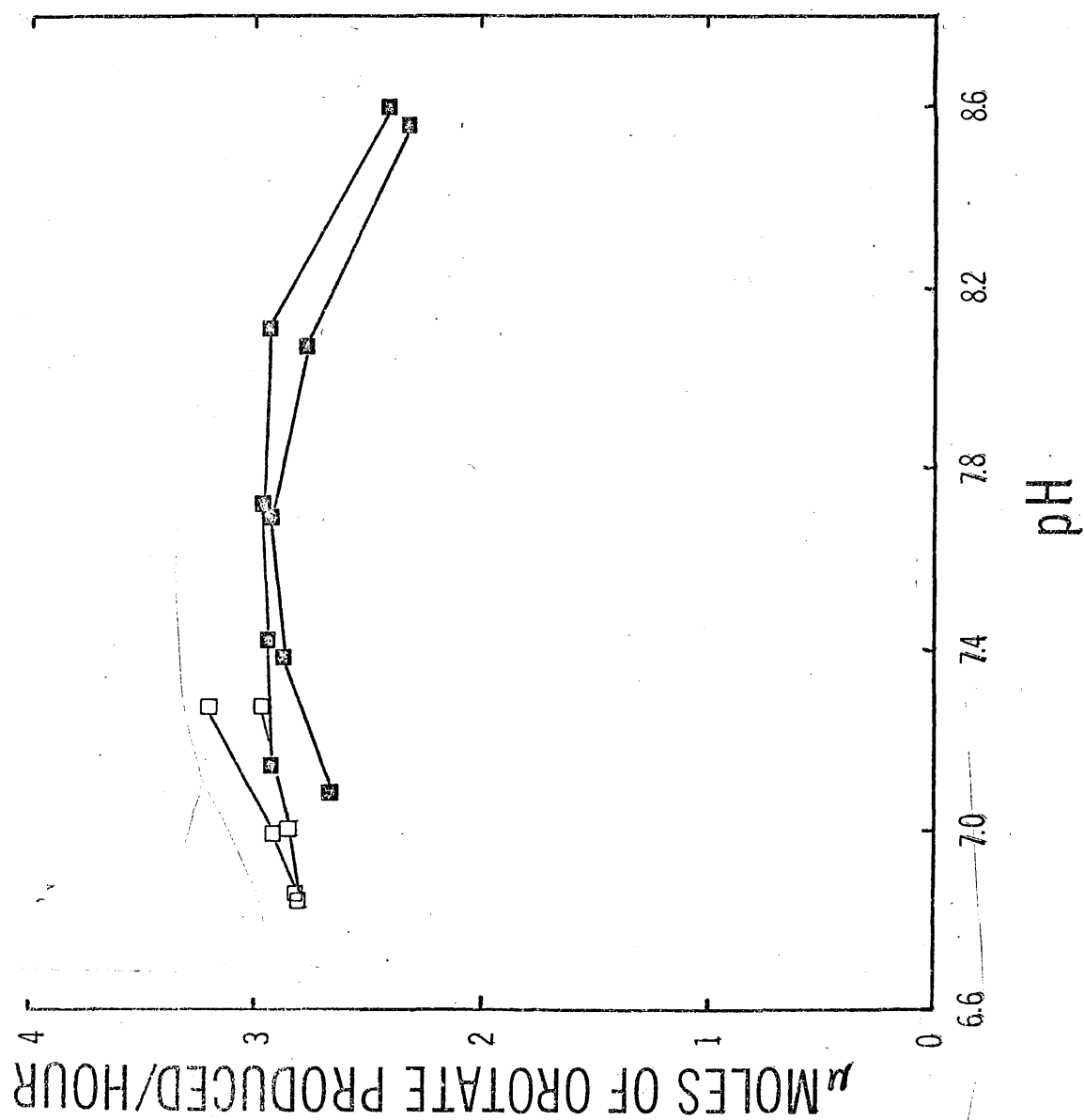


Figure 5. The effect of pH on biosynthetic dihydroorotate dehydrogenase activity.

The reaction mixture contained 300 μ moles of Tris-maleate buffer (pH 6.8 to 7.3) or Tris-HCl buffer (pH 7.2 to 8.6), 2 μ moles of potassium ferricyanide, 36 μ moles of sodium dihydroorotate, and 0.10 ml of a 1/100 dilution in AOV of a 3,800 unit/ml solution of enzyme (specific activity about 6,000 units/mg of protein). The reaction was initiated by adding enzyme in 1.0 ml of AV to the remaining reagents. Ferricyanide reduction was followed colorimetrically with a Klett-Summerson colorimeter (#42 filter) for 12 minutes. The pH of the reaction mixtures were measured at the end of the reaction period. Symbols: (\square), Tris-maleate buffer; (\blacksquare), Tris-HCl buffer.

Figure 6. The effect of orotate concentration on biosynthetic dihydroorotate dehydrogenase activity.

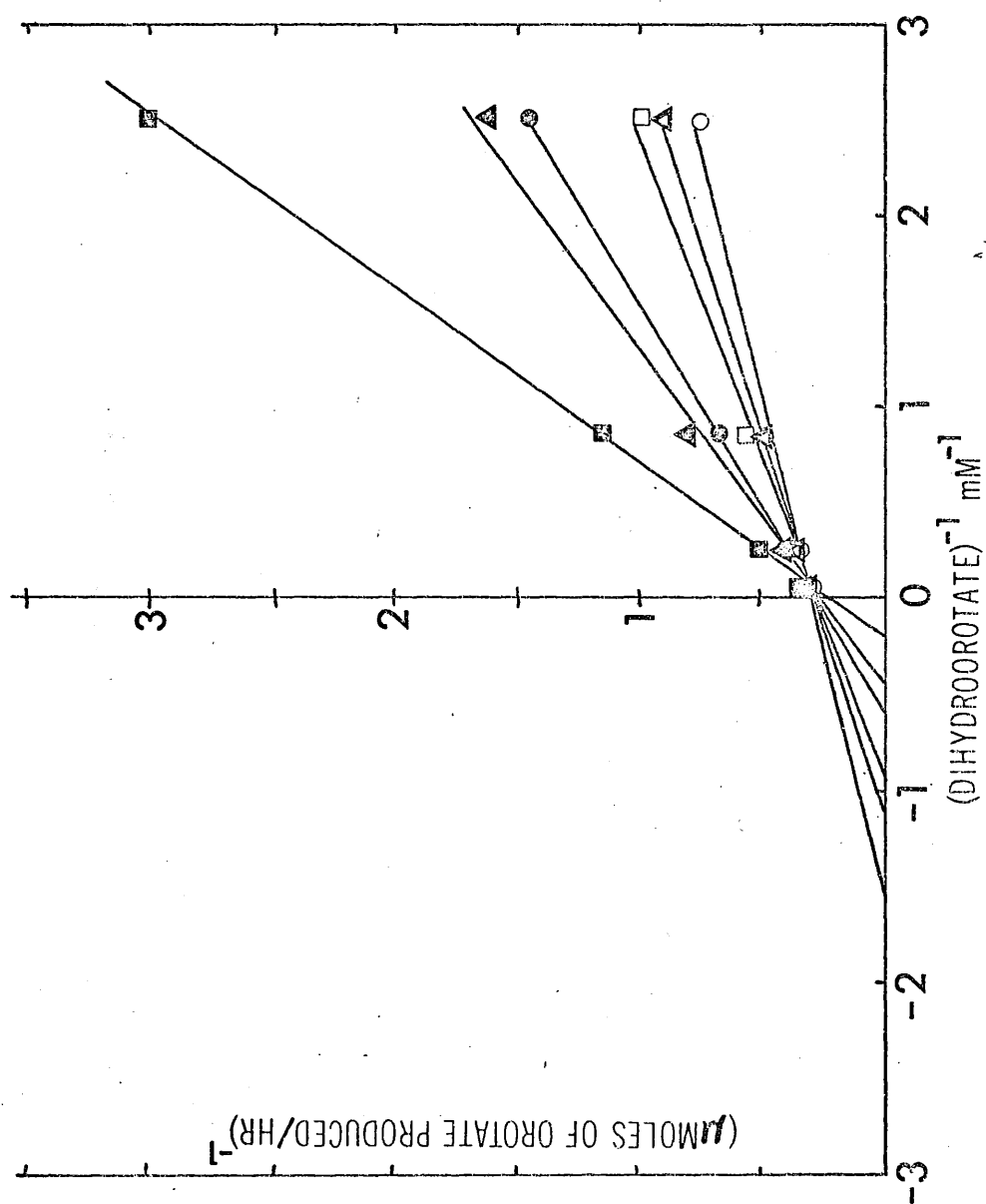


Figure 6. The effect of orotate concentration on biosynthetic dihydroorotate dehydrogenase activity.

The reaction mixture (3 ml) contained 300 μ moles of Tris-HCl buffer (pH 7.7), 2 μ moles of potassium ferricyanide, 1.2, 3.6, 12.0, or 48 μ moles of sodium dihydroorotate, 0.09, 0.24, 0.39, 0.69, 1.29, or 2.49 μ moles of sodium orotate, and 0.15 ml of a 1/100 in AOV of a 2960 unit/ml solution of enzyme (specific activity about 6,000 units/mg of protein). Several series of reactions were set up to obtain Lineweaver-Burk plots, each at a given orotate concentration, in which the DHO concentration varied from 0.4 to 16 mM. The reactions were initiated by adding enzyme, in 0.5 ml of AV, to the remaining reagents and followed colorimetrically with a Klett-Summerson colorimeter (#42 filter) for 12 minutes. Symbols: orotate concentration in the reaction mixture = (O), 0.030 mM; (Δ), 0.080 mM; (\square), 0.13 mM; (\bullet), 0.23 mM; (\blacktriangle), 0.43 mM; (\blacksquare), 0.83 mM.

from which the maximum velocity (V_{max}) is calculated. V_{max} is then plotted against pH. The pH optimum curves for DHO dehydrogenase prepared in this manner were found to be identical to those prepared under the conditions of Figure 5.

Determination of K_m for DHO and K_i for Orotate

The Lineweaver-Burk plot shown in Figure 6 shows that orotate is, as might be expected, a competitive inhibitor in the forward reaction (the oxidation of DHO) of DHO dehydrogenase. Because the apparent K_m increases with increasing concentration of a competitive inhibitor, the determination of the actual K_m is complicated by the presence of such compounds. This is the case with DHO dehydrogenase. Sodium orotate (0.6 mM) is present by necessity both in the concentrated Buchler electrophoresis fractions and in their dilutions which are used in the experiments. It can be shown from relations derived from basic concepts (43,44) (derivations in Appendix I) that the apparent K_m increases linearly with concentration of the competitive inhibitor. If this is the case then one should be able to plot the apparent K_m vs concentration of orotate and obtain a straight line which can be extrapolated to the actual K_m at zero concentration of orotate. Figure 7 shows the results of such a relationship from which an extrapolated K_m of 0.5 mM is obtained.

The K_i (inhibitor constant) for orotate was found to be about 0.1 mM by plotting $1/V_i$ vs $1/(S)$, $(S)/V_i$ vs (S) , calculating K_i from slope or intercept equations (44, p.151) and calculating for K_i from the data in Figure 5 utilizing relations derived in Appendix I.

Figure 7. The effect of orotate concentration on K_m for dihydro-orotate.

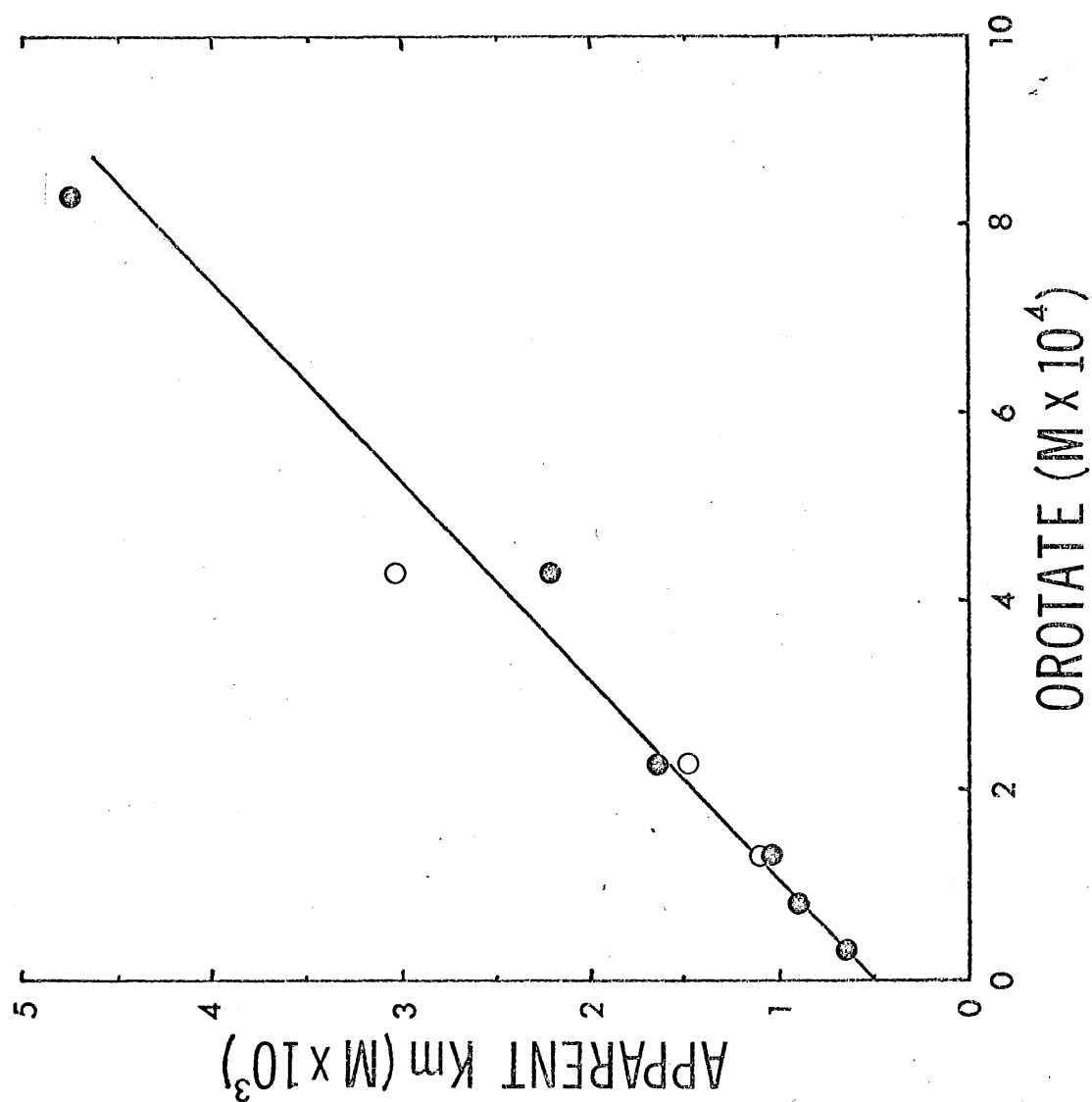


Figure 7. The effect of orotate concentration on K_m for dihydro-orotate.

The experimental conditions were identical to those of Figure 6.
Symbols: (●,○), represent results of two different experiments.

Effect of Ammonium Sulfate

In the development of the purification scheme it was discovered that the presence of ammonium sulfate markedly enhanced enzyme activity as measured by the ferricyanide reduction assay (26). Figure 8 shows that this effect increases with increasing concentrations of ammonium sulfate, saturating at about 1.4 M, and decreasing from that point on. As shown in Table IV equimolar concentrations of other salts exhibited similar but less marked stimulation than does ammonium sulfate.

Similar effects have been observed by other workers (45,46,42, p. 443). Massey found that the presence of various multivalent anions resulted in a shift of the alkaline branch of the pH optimum curve of fumarase further towards the alkaline range. The affinity of the enzyme for its substrate remained unaltered (46). He predicted that the anion binds to a basic group adjacent to the ionizable groups in the active site that determine the pH curve. Whether or not the group affected in the active site is acid or basic, the suppression of the adjacent positive charge will increase the pKa of the group, thus shifting the corresponding branch of the pH curve towards the alkaline. Another phenomenon was observed by Webb and Morrow (47) in which the height of the pH curve was increased in the presence of the anion. The form and positions of the curves did not change and there was no effect of the anion on the affinity of the enzyme for its substrate. They interpreted these results to mean that the anion directly effected the velocity constant of the breakdown of the enzyme-substrate (ES) complex to enzyme + product $(k_2)^1$.

Figure 8. The effect of ammonium sulfate on biosynthetic dihydroorotate dehydrogenase activity.

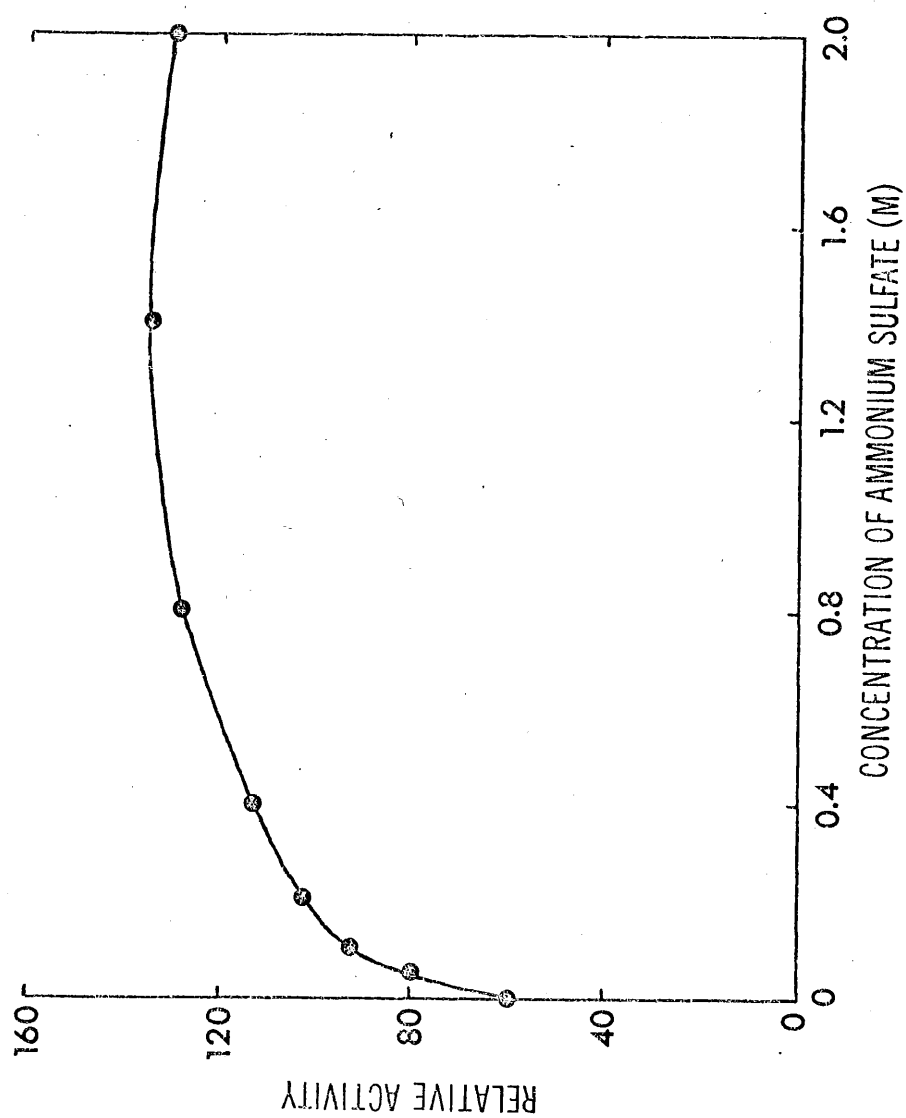


Figure 8. The effect of ammonium sulfate on biosynthetic dihydroorotate dehydrogenase activity.

The assay mixture (3 ml) contained 300 μ moles of Tris-HCl buffer (pH 7.8), 2 μ moles of potassium ferricyanide, 36 μ moles of sodium dihydroorotate, 0.00, 0.15, 0.30, 0.60, 1.20, 3.20, 4.20, or 6.00 mmoles of ammonium sulfate, and 0.10 ml of a 1/5 dilution in AOV of a 63 unit/ml solution of enzyme (specific activity about 1030 units/mg of protein). The reaction was initiated with ferricyanide and followed colorimetrically with a Klett-Summerson colorimeter (#42 filter) for 12 minutes.

TABLE IV
EFFECT OF SALTS ON BIOSYNTHETIC DIHYDROOROTATE
DEHYDROGENASE ACTIVITY

Salt added	Relative ionic strength	Relative activity
None	-	1.00
KCl	1	1.10
NaCl	1	1.14
MgCl ₂	3	1.16
NH ₄ Cl	1	1.27
Na ₂ SO ₄	3	1.33
MgSO ₄	4	1.35
K ₂ SO ₄	3	1.40
(NH ₄) ₂ SO ₄	3	1.70

The reaction mixture and procedure followed is described in Methods under the ferricyanide assay except that 500 μ moles of the indicated salt was also added. The enzyme consisted of 1.10 ml of a 37 unit/ml solution of combined Sephadex DEAE fractions (specific activity 156 units/mg of protein).

Figures 9 and 10 show the results of experiments performed to see if the ammonium sulfate stimulation of biosynthetic DHO dehydrogenase activity follows either of the two mechanisms discussed above. As can be seen from Figure 9, the presence of ammonium sulfate does not appear to markedly shift the position of the pH optimum, but rather exhibits an increase in the activity of the enzyme throughout the range of pH values tested. Figure 10 shows that the K_m for DHO is unaffected by the presence of ammonium sulfate. If the assumption that $K_m = k_{-1}/k_1$ is made and holds true with DHO dehydrogenase it can be interpreted that ammonium sulfate has no effect on the affinity of the enzyme for its substrate. It appears that the ammonium sulfate stimulation of DHO dehydrogenase would best be explained by the conclusions arrived at by Webb and Morrow (47), namely that the salt effects k_2 .

Effect of Sulfhydryl Inhibitors

Curve A of Figures 11 and 12 show the time course of inhibition of biosynthetic DHO dehydrogenase by the sulfhydryl inhibitors mercuric chloride and p-hydroxymercuribenzoate (p-HMB). These data suggest that if the sulfhydryl groups are not catalytically functional, they are at least located at or near the active site so that the mercaptide sterically or electrostatically inhibits the reaction. The rate of inhibition is quite slow, taking from 15 to 30 minutes to approach equilibrium inhibition. Since K_i is valid only at equilibrium conditions its determination for mercuric chloride and p-HMB would be tedious and probably

¹This interpretation was made under the assumption that of the relation $E + S \xrightleftharpoons[k_{-1}]{k_1} ES \xrightarrow{k_2} E + P$ (where E = enzyme, S = substrate, P = product, and k = rate constant) $K_m = k_{-1}/k_1$.

Figure 9. The effect of ammonium sulfate on the pH optimum of bio-synthetic dihydroorotate dehydrogenase.

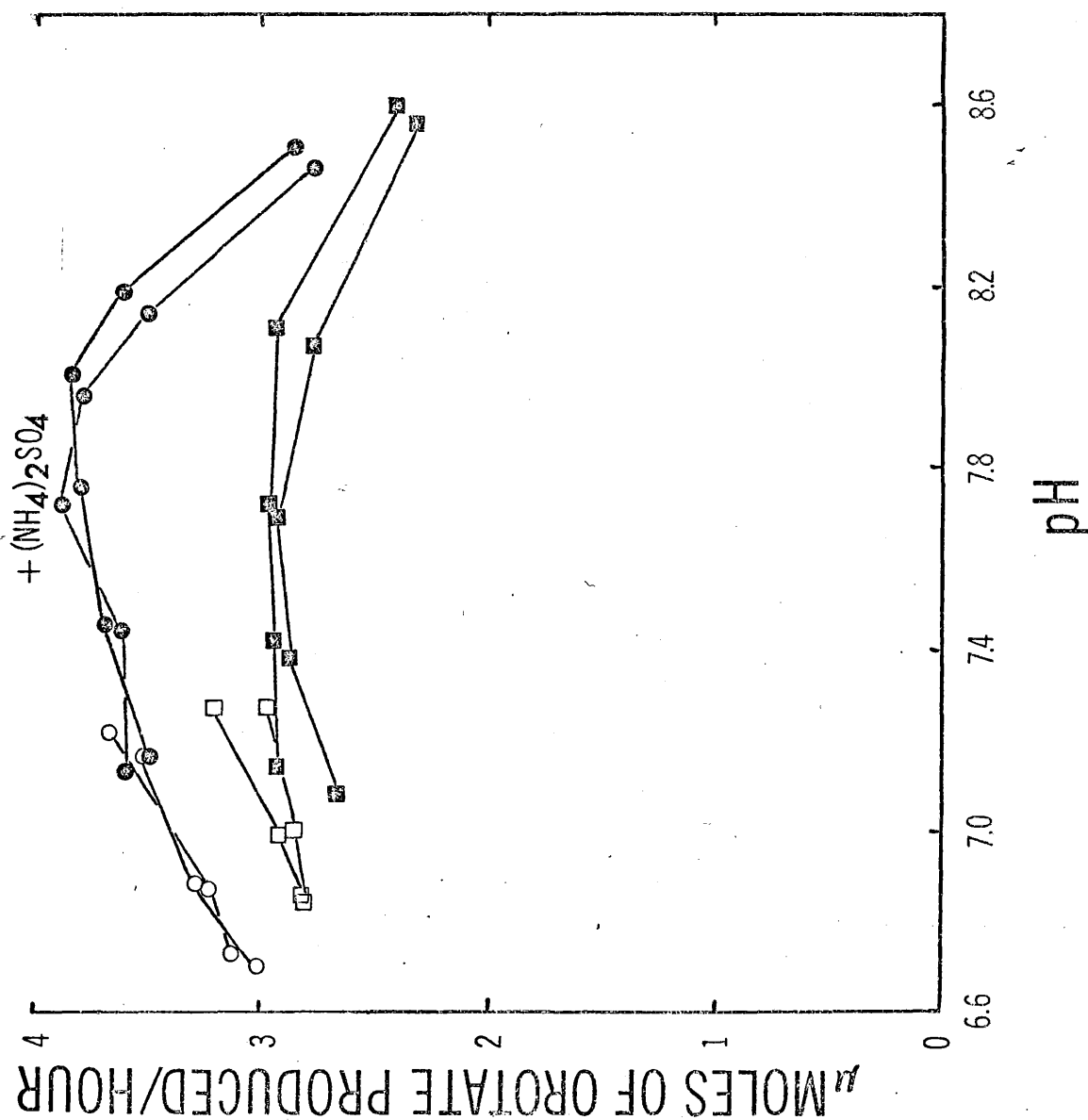


Figure 9. The effect of ammonium sulfate on the pH optimum of biosynthetic dihydroorotate dehydrogenase.

The reaction mixtures and procedures were identical to those in Figure 5 except that in the indicated curve, 500 μ moles of ammonium sulfate was also present. Symbols: (○,□), Tris-maleate buffer; (●,■), Tris-HCl buffer.

Figure 10. Effect of ammonium sulfate on the K_m for dihydroorotate.

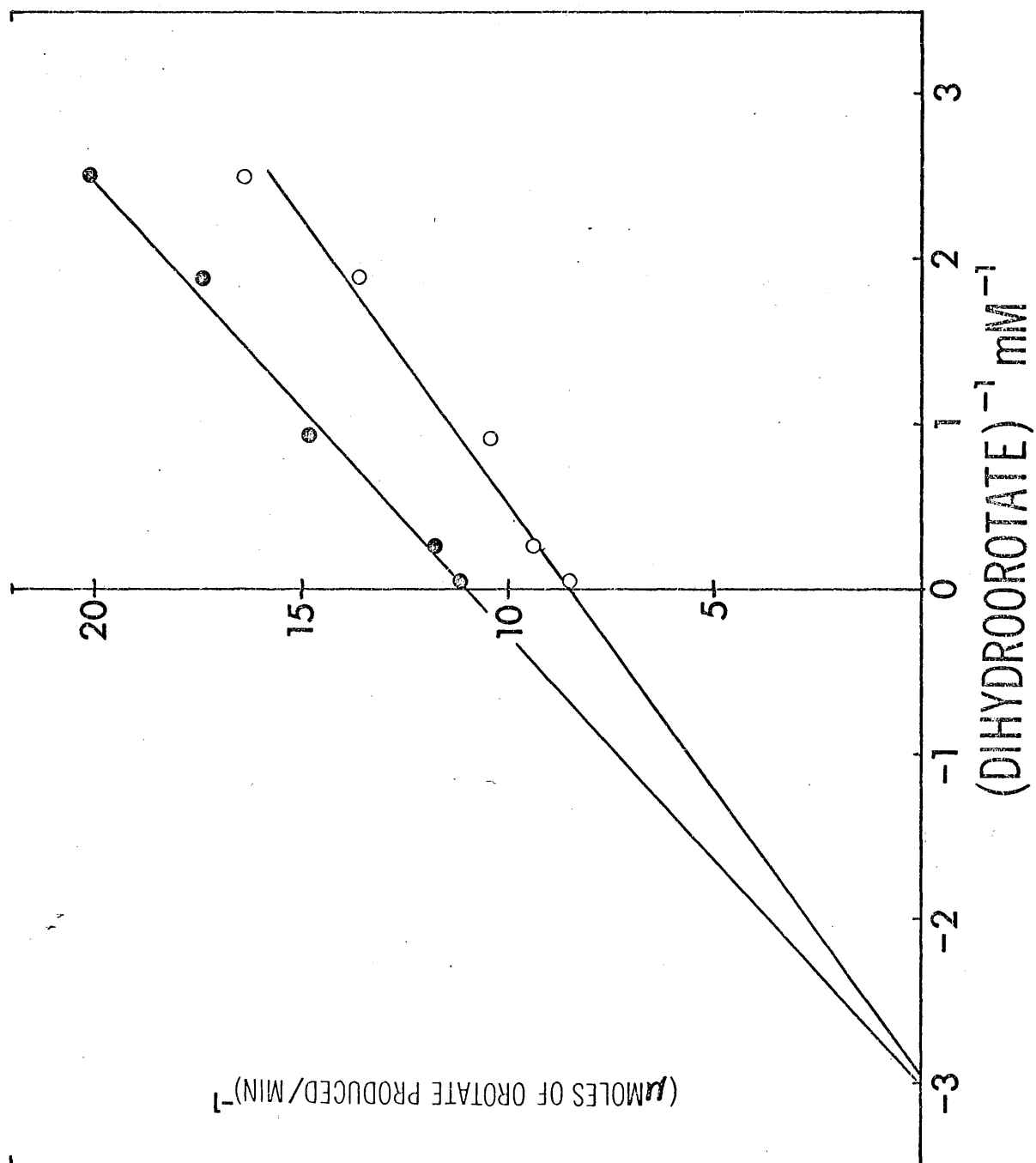


Figure 10. Effect of ammonium sulfate on the K_m for dihydroorotate.

The reaction mixture (3 ml) contained 300 μ moles of Tris-HCl buffer (pH 7.7), 2 μ moles of potassium ferricyanide, 1.20, 1.68, 3.60, 12.0, 48.0 μ moles of sodium dihydroorotate, 500 μ moles of ammonium sulfate (where indicated), and 0.10 ml of a 1/50 dilution in A0 of a 2,500 unit/ml solution of enzyme (specific activity about 5,000 units/mg of protein). The reaction was initiated by adding DHO and ferricyanide and followed spectrophotometrically in a Coleman Hitachi 124 at 420 nm for 3 minutes. Initial rates were used. Symbols: (O), ammonium sulfate present; (●), ammonium sulfate absent.

Figure 11. The effect of mercuric chloride on biosynthetic dihydroorotate dehydrogenase activity and protection by dihydroorotate.

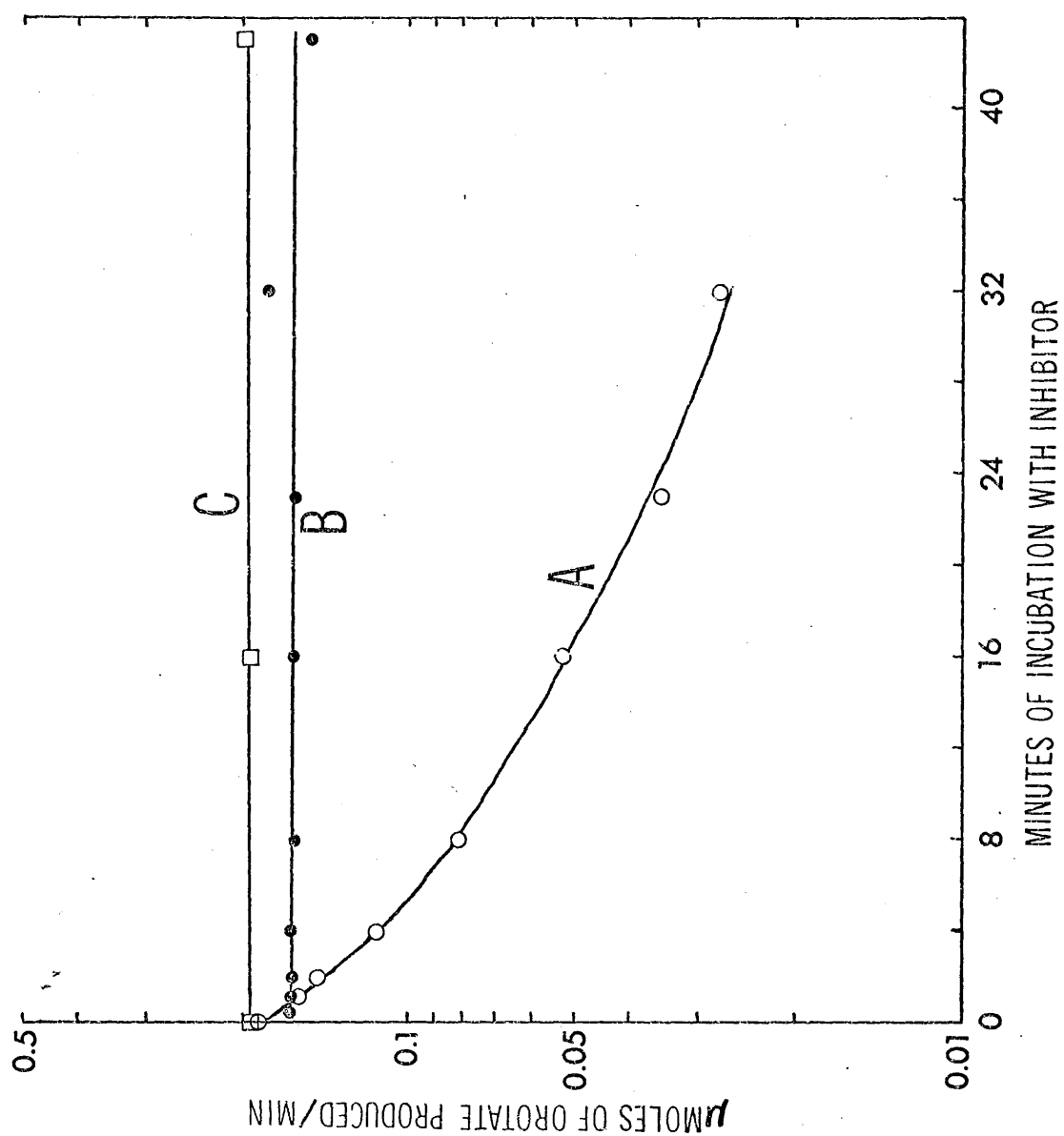


Figure 11. The effect of mercuric chloride on biosynthetic dihydroorotate dehydrogenase activity and protection by dihydroorotate.

The reaction mixtures (3 ml) contained 300 μ moles of Tris-HCl buffer (pH 7.7), 2 μ moles of potassium ferricyanide, 36 μ moles of sodium dihydroorotate, 0.1 nmoles of mercuric chloride, 0.20 ml of 1/50 dilution in AO of a 3,000 unit/ml solution of enzyme (specific activity about 6,000 units/mg of protein). The mixtures also contained 2 μ moles of acetate and 0.012 μ moles of orotate from carryover of AO with the enzyme. In curve A enzyme was added to the buffer and water followed by mercuric chloride (or water for the control, curve C) at specified times (volume 2.5 ml). This mixture was allowed to incubate at room temperature for various times and then the reaction initiated by adding DHO and potassium ferricyanide (0.5 ml total). In curve B (and its control) the DHO was present in the 2.5 ml incubation volume and the reaction initiated by adding ferricyanide and water (0.5 ml total). The reaction rates were followed spectrophotometrically in Coleman Hitachi 124 at 420 nm for three minutes.

Figure 12. The effect of p-hydroxymercuribenzoate on biosynthetic dihydroorotate dehydrogenase activity and protection by dihydroorotate.

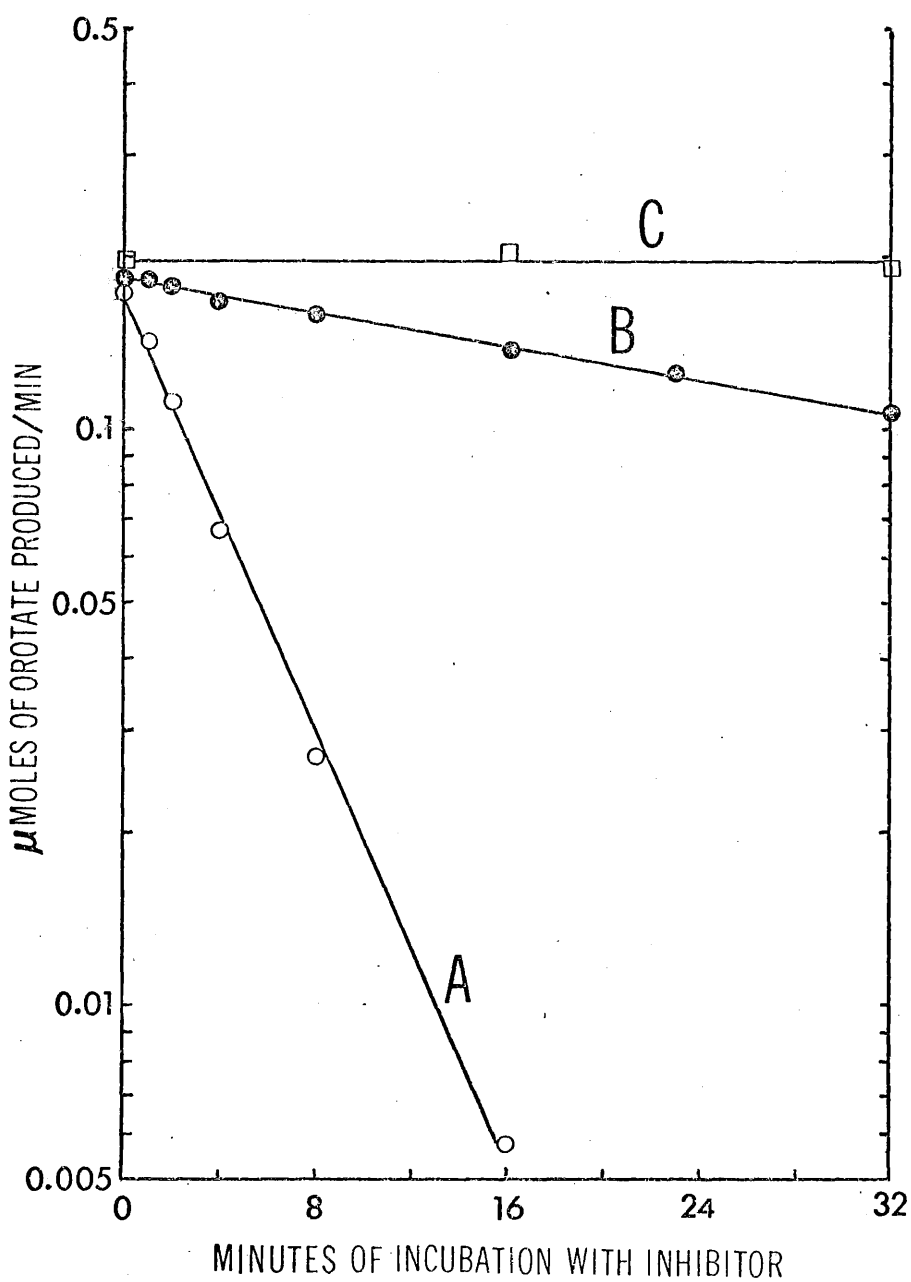


Figure 12. The effect of p-hydroxymecuribenzoate on biosynthetic dihydroorotate dehydrogenase activity and protection by dihydro-orotate.

The experimental conditions were identical to those in Figure 11 except that 5 nmoles of p-HMB were added in place of the mercuric chloride.

not accurate due to indeterminate secondary changes in the enzyme over the long incubation period. Such effects are evidenced in curve A of Figure 11 by the deviation from exponential decay of enzyme activity. A similar argument would stand for the difficulty of determining, by the method employed in Figure 6, whether these inhibitors are competitive or noncompetitive.

Curve B of Figures 11 and 12 shows that if the substrate DHO is present in the incubation mixture the rate of inhibition is very markedly decreased. This data is kinetic evidence that mercuric chloride and p-HMB are competitive inhibitors (44, p.552), providing further evidence that the sulfhydryl group resides within or very near the active site. Since orotate is a competitive inhibitor, rapidly reaching equilibrium inhibition, it would seem likely that its presence in low concentration would also protect the enzyme from sulfhydryl inhibition. Curve A of Figure 13 shows this to be the case with mercuric chloride up to an orotate concentration in the incubation mixture of about 0.45 mM. After this point orotate begins to inhibit more than protect. A similar but less marked effect is shown in curve B after incubation with mercuric chloride for 16 minutes. Curve C shows the degree of inhibition exhibited by orotate itself in the absence of mercuric chloride. Because of the small amount of orotate present in the enzyme solution for stability (which is therefore introduced into the reaction mixture) and the results in Figure 13, the absolute inhibition in Figures 11 and 12 are slightly less (4 to 5% or less) than would be expected if orotate were not present. However this should not alter any conclusions drawn from these data.

Figure 13. Protection of biosynthetic dihydroorotate dehydrogenase from mercuric chloride inhibition by orotate.

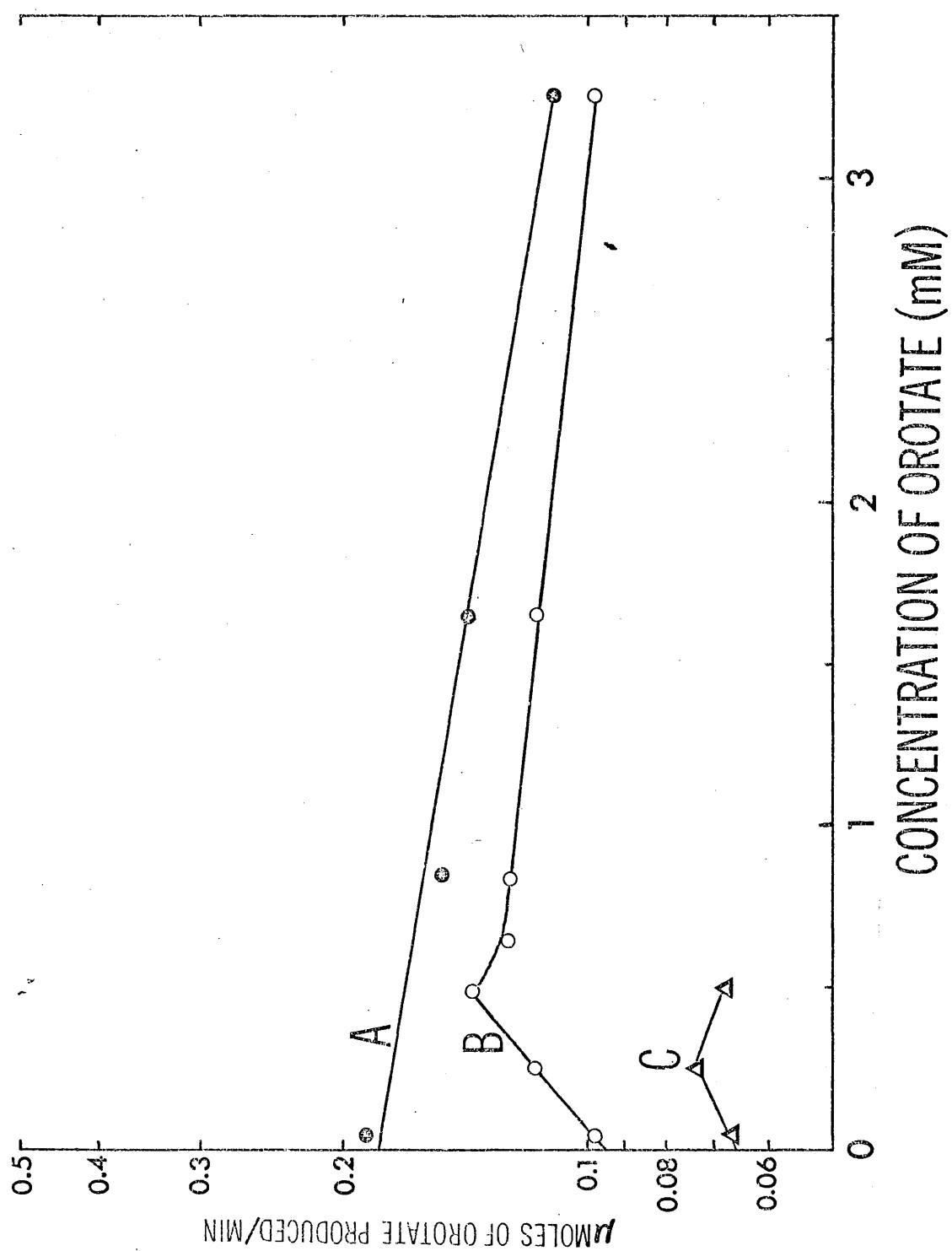


Figure 13. Protection of biosynthetic dihydroorotate dehydrogenase from mercuric chloride inhibition by orotate.

The reaction mixture (3 ml) consisted of 300 μ moles of Tris-HCl buffer (pH 7.7), 2 μ moles of potassium ferricyanide, 36 μ moles of sodium dihydroorotate, 0.1 nmoles of mercuric chloride, 0.20 ml of a 1/50 dilution in AO of a 3,000 unit/ml DHO dehydrogenase solution (specific activity about 6,000 units/mg of protein), and 0.50, 1.0, 1.5, 2.0, 4.0, or 8.0 μ moles of added sodium orotate. 0.012 additional μ moles of orotate as well as 2 μ moles of acetate were carried over with the enzyme. In curves A and B enzyme was added to the buffer, water, and a specified amount of orotate followed by mercuric chloride at a given time (volume 2.5 ml). This mixture was allowed to incubate for 5 minutes (curve A) and 16 minutes (curve B) before the reaction was initiated by adding DHO and potassium ferricyanide (0.5 ml total). The experimental conditions for curve C were the same as those for curve A except that water replaced mercuric chloride. The reaction rates were followed spectrophotometrically in a Coleman Hatachi 124 at 420 nm for three minutes.

Further evidence for the inhibition involving a sulfhydryl group is given in Table V. After the enzyme is inhibited to the level indicated, incubation with 0.175 mM mercaptoethanol for 3 minutes reversed inhibition to within 90% of full activity.

Indirect Evidence that Iron is Involved in Catalysis

Fridovich and Handler (48) found that the non-heme iron containing flavoprotein, xanthine oxidase, catalyzes substrate dependent sulfite autoxidation via a free radical reaction. They postulated that during normal catalysis iron served an electron transport function, resulting in a transient existence of the ferrous state (49) which could interact directly with oxygen, forming oxygen free radicals: $\text{Fe}^{+++} + \text{O}_2 \longrightarrow \text{Fe}^{++} + \cdot\text{O}_2^-$ (49). Several lines of evidence were presented supporting this postulate (50). Since that time non-heme iron containing and iron-free flavoproteins which are capable of reducing oxygen to hydrogen peroxide were tested for the ability to initiate sulfite autoxidation. However, to date only three are known to catalyze the reaction: xanthine oxidase, aldehyde oxidase (51), and catabolic DHO dehydrogenase (9), all of which are non-heme iron containing flavoproteins. All three have been shown to form an enzyme bound oxygen free radical by several criteria (52). Further evidence has led to the implication that the iron atoms in these three enzymes undergo identical valence changes and in fact may be bound to similar if not identical ligands (9). If biosynthetic DHO dehydrogenase demonstrates similar oxygen free radical formation, this would provide good indirect evidence that iron is present and that the mechanism of its action might be similar or identical to that

TABLE V
REVERSAL OF SULFHYDRYL INHIBITION
BY MERCAPTOETHANOL

Inhibitor used	Treatment			
	A) Inhibitor	B) Inhibitor followed by mercapto- ethanol	C) No inhibitor	D) No inhibitor mercaptoethanol present
	μ moles DHO oxidized/min	μ moles DHO oxidized/min	μ moles DHO oxidized/min	μ moles DHO oxidized/min
HgCl ₂	0.0991	0.147	-----	-----
pHMB	0.00437	0.151	-----	-----
None	-----	-----	0.171 ^{a,b}	0.163 ^a 0.167 ^b

The reaction mixture (3 ml) contained 300 μ moles of Tris-HCl buffer (pH 7.7), 2 μ moles of potassium ferricyanide, 36 μ moles of sodium dihydrooxotrate, 5 nmoles of p-HMB or 0.1 nmoles of mercuric chloride, 0.20 ml of a 1/50 dilution in AO of a 3,000 unit/ml solution of enzyme (specific activity about 6,000 units/mg of protein), and 0.438 μ moles of mercaptoethanol (where added). The inhibited and control rates (A and C) were obtained by a procedure identical to that used in curve A of Figures 11 and 12 except that the incubation volume was 2.2 ml and the incubation time with inhibitor was set at 5 minutes for p-HMB, 15 minutes for mercuric chloride. The reaction rate of B was obtained by incubating enzyme, buffer and water with inhibitor (incubation volume was 2.2 ml) for the specified time, adding mercaptoethanol, and allowing the mixture (2.5 ml) to incubate three minutes. The reaction was then initiated by adding DHO and ferricyanide (0.5 ml). Rate D was obtained in the same manner except that water replaced inhibitor. The enzyme was incubated in the buffer and water mixture (total volume 2.2 ml) for ^a 15 minutes, ^b 5 minutes.

of the three other extensively studied iron flavoproteins. Figure 14 shows results typical to substrate dependent, enzyme catalyzed sulfite autoxidation. The greatly amplified oxygen uptake over that in which sulfite is absent, and the quenching of the sulfite dependent oxygen uptake by the presence of a free radical "scavenger," mannitol, suggests that the biosynthetic DHO dehydrogenase-catalyzed reaction does indeed proceed by a free radical mechanism. Figure 14 shows that the ferric iron ligand Tiron (disodium 1,2-dihydroxybenzene-3,5-disulfonate) markedly inhibits sulfite autoxidation, a phenomenon also observed with catabolic DHO dehydrogenase (9), providing further evidence that iron may be involved in oxygen free radical formation.

This laboratory has also demonstrated the presence of iron in biosynthetic DHO dehydrogenase (26) by the use of the o-phenanthroline assay of Massey (53) in which the colored ferrous iron-o-phenanthroline chelate was measured spectrophotometrically.

Evidence Relating to the Flow of Electrons in Biosynthetic DHO Dehydrogenase

In active site studies, Fridovich and Handler with xanthine oxidase (49,54) and Aleman and Handler with catabolic DHO dehydrogenase (9) found that dye reduction and reduction of oxygen to hydrogen peroxide responded differently to various inhibitors than did oxygen reduction to a free radical or the very closely related reduction of cytochrome c. The study of these differences allowed the workers to sketch tentative schemes for the internal electron transport and to predict that the various modes of reduction may occur at different sites.

Figure 14. Initiation of sulfite autoxidation by biosynthetic dihydroorotate dehydrogenase.

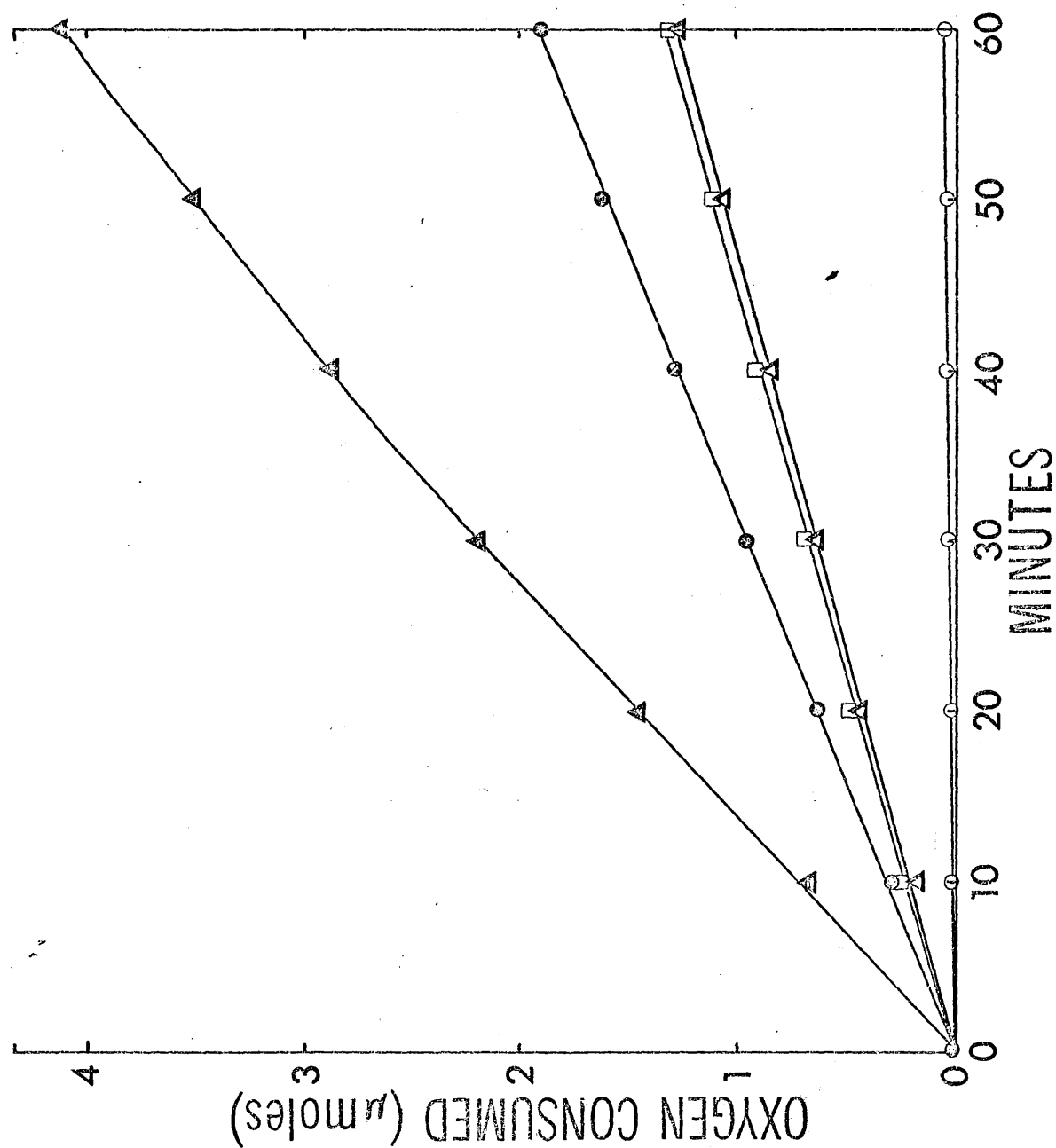


Figure 14. Initiation of sulfite autoxidation by biosynthetic dihydrooorotate dehydrogenase.

The reaction mixture (2 ml) consisted of 200 μ moles of potassium phosphate buffer (pH 7.7), 2 μ moles of EDTA, 24 μ moles of sodium dihydrooorotate, 100 μ moles of sodium sulfite, 0.2 ml of a 1/50 dilution in AO of a 3,000 unit/ml solution of enzyme (specific activity about 6,000 units/mg of protein), and (where indicated) 300 μ moles of mannitol, 0.5 or 0.1 μ moles of Tiron. Control mixtures were identical except that DHO was replaced by water. The reactions were initiated by tipping in enzyme and sulfite from separate side arms and the oxygen consumption measured in a Gilson differential respirometer. Symbols: (Δ), sulfite present; (\odot), sulfite + 0.25 mM Tiron present; (\square), sulfite + 0.50 mM Tiron present; (\circ), no sulfite present; (\triangle), mannitol present.

Evidence thus far presented has shown that biosynthetic DHO dehydrogenase is capable of oxidizing DHO to orotate using as electron acceptors, oxygen (26), via a two electron transfer yielding hydrogen peroxide (Figure 3) or a free radical mechanism (Figure 14), various redox dyes such as potassium ferricyanide (21), p-nitro blue tetrazolium (26), and as will be shown, cytochrome c and DCI (Table VI). Since the electrons reducing the various acceptors are most likely derived from at least two sources (FMN and iron) it is possible that differences in behavior with various inhibitors will allow some discussion as to the scheme of the internal electron transport of biosynthetic DHO dehydrogenase.

Table VI shows the effect of p-HMB, a sulfhydryl inhibitor, and Tiron, a ferric iron chelator, on the reaction rate of biosynthetic DHO dehydrogenase in the presence of ferricyanide, DCI, oxygen, or cytochrome c as the electron acceptor. The effect of Tiron on sulfite autoxidation is also shown. All activities tested were found to be inhibited by p-HMB, but only cytochrome c reduction and sulfite autoxidation were inhibited by Tiron. The inhibition of ferricyanide reduction by Tiron could not be measured and the measurement of the inhibition of sulfite autoxidation by p-HMB was complicated by the quenching of the free radical reaction by the organic constituents in the reaction mixture. The inhibition of cytochrome c by Tiron must be interpreted with care. Miller and Massey (55) have postulated that the observed Tiron inhibition may be due, at least in part, to the reoxidation of reduced cytochrome c by Tiron. However, Aleman and Handler in a later paper (9) did not mention such a phenomenon when reporting their inhibition data. As

TABLE VI

EFFECT OF TIRON AND p-HYDROXYMERCURIBENZOATE
ON DIHYDROOROTATE DEHYDROGENASE ACTIVITY
WITH VARIOUS ELECTRON ACCEPTORS

Acceptor or sub- stance oxidized	Inhibitor			
	p-HMB		Tiron	
	Concentration of inhibitor	Inhibition	Concentration of inhibitor	Inhibition
	μM	%	mM	%
FeCN	2.0	75	-----	-----
DCI	2.0	80	1.2	3.3
			2.4	3.8
Oxygen	1.0	60	0.40	6.0
			1.2	4.0
Cytochrome c	2.0	40	0.33	27
	6.0	83	0.66	54
Sulfite	---	---	0.25	47
autooxidation			0.50	72

The reaction mixtures (3 ml) contained 300 μmoles of Tris-HCl buffer (pH 7.7), 2 μmoles of potassium ferricyanide, 0.2 μmoles of DCI, 1 mg of cytochrome c, or no added acceptor, 36 μmoles of sodium dihydroorotate, the specified amounts of inhibitor (not present in the controls), 0.2 ml of a 1/50 dilution in AO of a 3,000 unit/ml solution of enzyme (specific activity about 6,000 units/mg of protein) was used in the cytochrome c assay. The enzyme was added to the buffer and water followed by given amounts of inhibitor at a specific time. This mixture (2.5 ml) was allowed to incubate 5 minutes and the reaction initiated by the addition of DHO and acceptor (0.5 ml), DHO and water (0.5 ml) when oxygen was used as the acceptor. The experimental conditions of the measurement of sulfite autooxidation was as stated in Figure 14.

Ferricyanide and DCI reduction was followed spectrophotometrically at 420 nm and 600 nm respectively, using a blank consisting of buffer, DHO, and water. Orotate production (acceptor, oxygen) was followed at 282 nm using a blank containing buffer, enzyme, water, and Tiron equivalent to that to that used in the reaction mixtures (p-HMB does not absorb at this wavelength). Cytochrome c reduction was followed at 550 nm with a blank consisting of buffer, DHO, cytochrome c and water. Sulfite autooxidation was measured as stated in Figure 14.

admitted by Miller and Massey (55), however, this possible artifact does not explain the observed inhibition of sulfite autoxidation by Tiron. Since these two processes proceed via the same mechanism (oxygen free radical formation) it is possible that cytochrome c reduction is indeed inhibited by Tiron, but the observed decreases in activity are also partially due to the above mentioned artifact.

These results suggest that the sulfhydryl inhibitor blocks electron transfer early in the reaction sequence, presumably by a mechanism which prevents the binding of the substrate, or which interferes with the transfer of electrons from an initial acceptor to one succeeding. The fact that Tiron only inhibits sulfite autoxidation and (probably) cytochrome c reduction, which is mediated by an oxygen free radical bridge between the enzyme and acceptor (54,52) suggests that either the iron groups are reduced subsequent to the reduction of the flavin, or Tiron specifically inhibits oxygen free radical formation, not affecting a possible electron transport function of the iron.

Reduction of Various Electron Acceptors by Dihydroorotate Dehydrogenase

Table VII allows a comparison of the rates of reaction exhibited by DHO dehydrogenase using several different electron acceptors. Under the conditions employed the redox dyes exhibit the most rapid reaction, oxygen and cytochrome c being far less efficient. This general occurrence was also found with catabolic DHO dehydrogenase (6,55,9).

TABLE VII

RATE OF OXIDATION OF DIHYDROOROTATE TO OROTATE BY BIOSYNTHETIC
DIHYDROOROTATE DEHYDROGENASE USING VARIOUS
ELECTRON ACCEPTORS

<u>Acceptor</u>	<u>Reaction rate</u> μ moles DHO oxid/min/ml of enzyme
Ferricyanide	52.5
DCI	75.0
Oxygen	2.5
Cytochrome c	0.89

The experimental conditions were identical to those of Table V except that inhibitor was not present. Standard curves were prepared to relate change in absorbance to total μ moles of DHO oxidized in a reaction mixture of 3 ml.

DISCUSSION

Internal Electron Transport

Catabolic DHO Dehydrogenase. Figure 15 represents the internal electron transport scheme of catabolic DHO dehydrogenase proposed by Aleman and Handler (9). Quantitative determinations have shown that

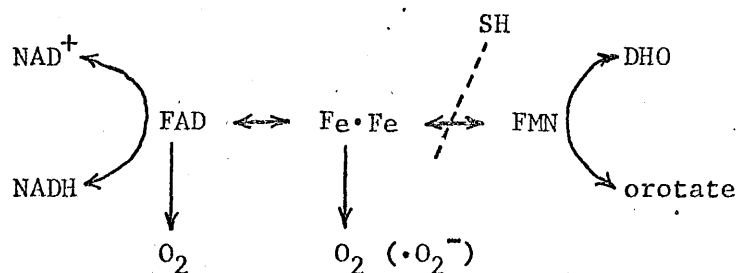


Figure 15. Internal electron transport in catabolic dihydroorotate dehydrogenase.

both FMN and FAD are present in the enzyme along with non-heme iron and labile sulfhydryl groups (7,8,9). The flavins function as intermediate electron carriers as shown by the fact that under anaerobic conditions they were bleached¹ by varying degrees upon the addition of either DHO or NADH. The demonstration of a stable enzyme-orotate complex and observed decreases in fluorescence upon addition of orotate characteristic of those occurring when compounds bind to free FMN, suggest that FMN is the binding site and the immediate electron donor for orotate. It was predicted that the FAD moiety serves as the first

¹Bleaching of flavins is an occurrence characteristic of their reduction and consists of extensive decreases in extinction usually measured at the 450 nm absorption peak.

electron acceptor for NADH (9). Iron was found to serve as an intermediate electron carrier from several lines of evidence including behavior of flavin-free iron protein derived from the enzyme, an electron paramagnetic resonance signal typical of reduced iron, and the presence of free radical reactions occurring at the iron site (9). The catabolic enzyme exhibits a marked cysteine activation (5,6,7,9) and p-chloromercuribenzoate (p-CMB) inhibition (9) of the activities involving DHO or orotate. Also, the fact that the NADH oxidase activity is unaffected by these compounds suggests that a sulfhydryl group on the enzyme must be in the reduced condition before the flavin at the DHO-orotate site can transfer electrons to or receive electrons from the iron site. These data also suggest that the FMN at the DHO-orotate site is not autoxidizable. The formation of oxygen-free radicals has been shown to occur at the iron residue.

Xanthine Oxidase. The internal electron transport scheme proposed by Fridovich and Handler (49,50) is shown in Figure 16. Though dif-

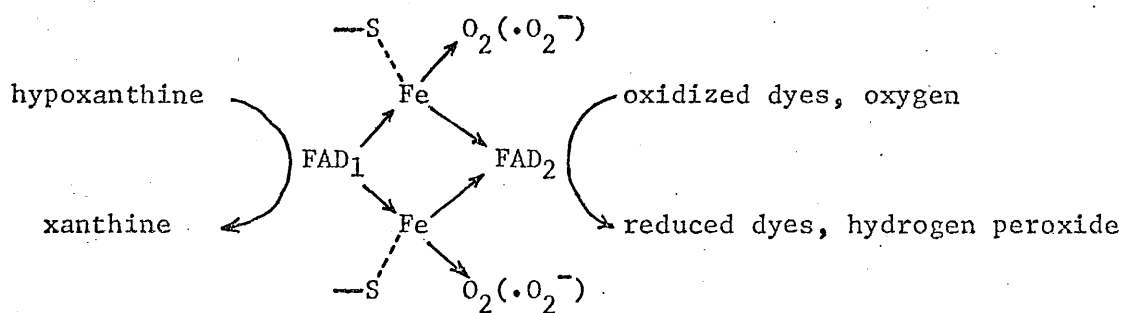


Figure 16. Internal electron transport in xanthine oxidase.

ferent in some respects, this scheme is quite analogous to that of catabolic DHO dehydrogenase. The substrate hypoxanthine has been shown to bind specifically to flavin-1 from which the electrons are transferred

via ferric mercaptide groups to flavin-2, and from there to oxygen or other acceptors. Binding of hypoxanthine to flavin-2 can be induced by the presence of a large excess of the substrate and results in an inhibition of the processes carried out by that moiety. Excess substrate inhibition of the aerobic oxidation of hypoxanthine demonstrated that flavin-1, like the FMN of catabolic DHO dehydrogenase, is not autooxidizable. Likewise cyanide and p-CMB interfered with the ability of the iron complex to transfer electrons from the first to the second flavin. The enzyme was also found to initiate the reduction of oxygen to a free radical.

Biosynthetic DHO Dehydrogenase. Since catabolic DHO dehydrogenase and xanthine oxidase are similar in several respects it is possible that, in light of the properties shown, biosynthetic DHO dehydrogenase may follow a similar scheme of internal electron transport. Though verification awaits detailed studies of the physical and functional nature of the biosynthetic enzyme the proposed electron transport scheme of Figure 17 is consistent with the data presented in Results. It has

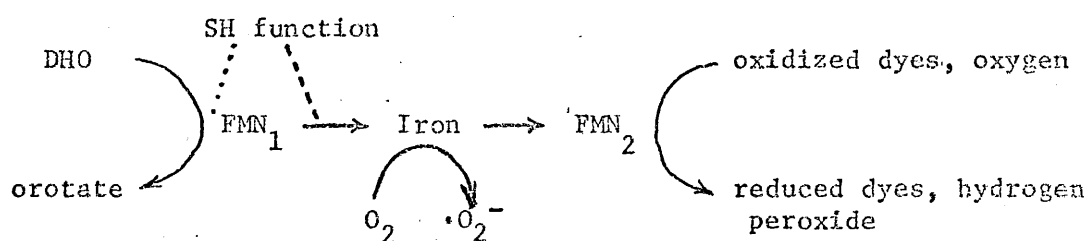


Figure 17. Proposed sequence of internal electron transport in biosynthetic dihydroorotic dehydrogenase.

been shown directly that biosynthetic DHO dehydrogenase is an FMN-containing flavoprotein (Figure 4, Tables II and III) and indirectly that

FMN and iron are reduced during the oxidation of DHO to orotate (Figures 3 and 14). A functional sulfhydryl moiety is necessary for activity (Figures 11 and 12, Table V) and inactivation of the group(s) halts electron transport early in the sequence (Table VI). With the evidence thus far obtained, the sulfhydryl group(s) function in one of the following ways: 1) binding of DHO to the enzyme, 2) electron transfer between DHO and flavin-1, or 3) the transfer of electrons between flavin-1 and the iron complex. It is logical to predict that alternative 3) exists with biosynthetic DHO dehydrogenase by analogy with the catabolic enzyme and xanthine oxidase. In these enzymes the sulfhydryl moieties function in the transfer of electrons from the primary flavin to the iron complex, while substrates bind to the flavin moieties without sulfhydryl participation. To verify alternative 3) for the biosynthetic enzyme, studies will have to be done to show that with p-HMB inactivated enzyme DHO still binds to the enzyme and reduces the primary flavin. If the sulfhydryl function is as predicted the results presented in Table VI (the p-HMB inhibition of dye reduction and DHO oxidase activity) suggest that flavin-1 is not capable of transferring electrons to the terminal acceptors, but rather transfers electrons to an intermediate carrier. It is possible that iron functions as the intermediate carrier, passing electrons from flavin-1 to a second flavin from which dyes and oxygen are reduced.

The observation that Tiron specifically inhibits sulfite autooxidation (Table VI) has also been reported for xanthine oxidase (54). A possible explanation of this finding may be that chelation of the iron by Tiron renders the site of free radical formation unavailable

to oxygen, sulfite, or cytochrome c, but does not significantly alter the ability of iron to transfer electrons to flavins.

Comparison of Catabolic and Biosynthetic DHO Dehydrogenase

Table VIII outlines the major physical and kinetic properties determined for catabolic and biosynthetic DHO dehydrogenase. Because of the availability of only low concentrations of the biosynthetic enzyme several determinations such as flavin, iron and sulfhydryl content have not been made on a quantitative basis. The striking differences between the two enzymes is in the area of molecular weight, flavin content, and pyridine nucleotide-linked activities. Biosynthetic DHO dehydrogenase has a molecular weight roughly one half that of the catabolic enzyme and does not contain either FAD or the associated pyridine nucleotide-linked activities. In contrast to the catabolic enzyme, biosynthetic DHO dehydrogenase does not exhibit stimulation by cysteine or mercaptoethanol. The two enzymes appear to be similar in all other respects except perhaps in terms of K_m .

It is interesting to note that in high concentrations of guanidine hydrochloride catabolic DHO dehydrogenase dissociates into four subunits with molecular weights of 30,000 to 31,000 each. Since there are four gram atoms of iron per mole of enzyme it was predicted that the enzyme was a tetramer (17). Since upon dissociation both flavin and iron are released it is to date not possible to determine neither the prosthetic group content nor how they were attached. However it is not unreasonable to predict that each subunit contains a flavin and an iron moiety, two involving FMN and two involving FAD. In light of the evidence relating

TABLE VIII
 PROPERTIES OF CATABOLIC AND BIOSYNTHETIC
 DIHYDROOROTATE DEHYDROGENASE

Property	Catabolic DHO dehydrogenase	Biosynthetic DHO dehydrogenase
Molecular weight	115,000 \pm 7,000 (9) 112,000 to 124,000 (17)	53,000 to 57,000 (26)
Number of subunits	4 (17)	2?
Flavin content	2 moles FAD, 2 moles FMN per mole of enzyme (9)	FMN
Sulfhydryl content	4 moles per mole of enzyme (9)	present
Iron content	4 gram atoms per mole of enzyme (9)	present
Oxidation of NADH or NADPH by orotate and oxygen	+ (6,18)	-- (21,22,26)
Oxidation of DHO by:		
DPN ⁺	+ (6)	-- (21,22,26)
Oxygen	+ (6)	+
Redox dyes	+ (9)	+
Demonstrates oxygen free radical forma- tion	+ (9)	+
Km for DHO	0.18 mM, acceptor oxygen (8) 0.18 mM, acceptor NAD ⁺ (9)	0.3 to 0.5 mM, acceptor ferricyanide
Km,Ki for orotate	Km = 2.9 uM, electron donor NADH (9) 1.8 mM, electron donor NADH (8)	Ki = 0.1 mM
pH optimum	pH 8.2 for reduction of NAD ⁺ by dihydroorotate and dihydroorotate oxidase activity	pH 7.6 to 7.8 for oxi- dation of DHO by ferricyanide

to the molecular weight, flavin content, and lack of pyridine nucleotide-linked activities of biosynthetic DHO dehydrogenase (Table VIII) it is tempting to speculate that the biosynthetic enzyme is a dimer, consisting of FMN and iron-containing subunits, and that the catabolic enzyme is formed by the addition of two more FAD containing subunits to support the pyridine nucleotide-linked reduction of orotate to DHO. However, to date no evidence has been provided to support such an occurrence. Studies with mutants would be especially valuable in this regard.

SUMMARY

1. Biosynthetic dihydroorotate dehydrogenase was isolated in an extensively purified form from Lactobacillus bulgaricus.
2. Kinetic studies were carried out including the determination of the K_m for dihydroorotate, K_i for orotate, pH optimum, and the behavior of the enzyme in response to sulfhydryl inhibitors and ammonium sulfate.
3. The enzyme was found to contain FMN and indirect evidence shows that iron is also present. Inhibitor studies have shown that a group must be in the reduced sulfhydryl form in order for the enzyme to function.
4. A possible scheme of internal electron transport for biosynthetic DHO dehydrogenase is presented.
5. A comparison between catabolic and biosynthetic DHO dehydrogenase is made on the basis of physical and kinetic properties.

REFERENCES

1. Lieberman, I., and A. Kornberg, J. Biol. Chem. 207:911 (1954).
2. Lieberman, I., and A. Kornberg, J. Biol. Chem. 212:909 (1955).
3. Reynolds, E.S., I. Lieberman, and A. Kornberg, J. Bacteriol. 69:250 (1955).
4. Mahler, H.R., and E.H. Cordes, (eds), Biological Chemistry, Harper and Row Publishers, New York: 1966.
5. Lieberman, I., and A. Kornberg, Biochemica Et Biophys Acta, 12:223 (1953).
6. Friedmann, H.C., and B. Vennesland, J. Biol. Chem. 233:1398 (1958).
7. Friedmann, H.C., and B. Vennesland, J. Biol. Chem. 235:1526 (1960).
8. Miller, R.W., and V. Massey, J. Biol. Chem. 240:1453 (1965).
9. Aleman, V., and P. Handler, J. Biol. Chem. 242:4087 (1967).
10. Krakow, G., and B. Vennesland, J. Biol. Chem. 236:142 (1961).
11. Aleman, V., and P. Handler, J. Biol. Chem. 243:2560 (1968).
12. Aleman, V., and P. Handler, J. Biol. Chem. 243:2569 (1968).
13. Handler, P., K.V. Rajagopalan, and V. Aleman, Fed. Proc. 23:30 (1964).
14. Aleman, V., S.T. Smith, K.V. Rajagopalan, and P. Handler in A. San Pietro, (ed), Non-heme Iron Proteins: Role in Energy Conversion, The Antioch Press, Ohio: 1965, 237.
15. Aleman V., K.V. Rajagopalan, P. Handler, H. Beinert, and G. Palmer, in H.S. Mason, T.E. King, and M. Morrison, (eds), Oxidases and Related Redox Systems, Vol. I, John Wiley and Sons, Inc. New York: 1964, 380.
16. Aleman V., S.T. Smith, K.V. Rajagopalan, and P. Handler in E.C. Slater, (ed), Flavins and Flavoproteins, Elsevier Publishing Co. London: 1966, 99.
17. Nelson, C.A., and P. Handler, J. Biol. Chem. 243:5368 (1968).

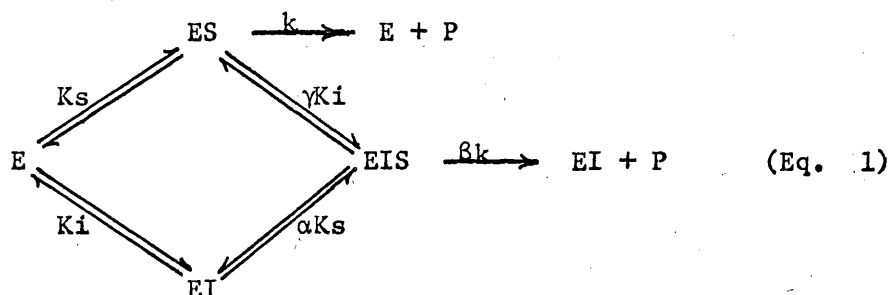
18. Udaka, S., and B. Vennesland, J. Biol. Chem. 237:2018 (1962).
19. Yates, R.A., and A.B. Pardee, J. Biol. Chem. 221:743 (1956).
20. Yates, R.A., and A.B. Pardee, J. Biol. Chem. 227:677 (1957).
21. Taylor, W.H., and M.L. Taylor, J. Bacteriol. 88:105 (1964).
22. Taylor, W.H., M.L. Taylor, and D.F. Eames, J. Bacteriol. 91:2251 (1966).
23. Kerr, C.T., and R.W. Miller, Canadian J. of Biochem. 45:1295 (1967).
24. Kerr, C.T., and R.W. Miller, Canadian J. of Biochem. 45:1283 (1967).
25. Wright, L.D., C.S. Miller, H.R. Skeggs, J.W. Huff, L.L. Weed, and D.W. Wilson, J. Amer. Chem. Soc. 73:1898 (1951).
26. Taylor, W.H., M.L. Taylor, D.F. Eames, and C.D. Taylor, Manuscript in Preparation.
27. Wright, L.D., C.A. Driscoll, C.S. Miller, H.R., Skeggs, Proc. Soc. Exp. Biol. Med., 84:716 (1953).
28. Jovin, T., A. Chrambach, and M.A. Naughton, Anal. Biochem. 9:351 (1964).
29. Haas, E., B.L. Horecker, and T.R. Hogness, J. Biol. Chem. 136:747 (1940).
30. Burton, K. in Colowick, S.P. and N.O. Kaplan, (eds), Methods of Enzymology, Vol. II, Academic Press, New York: 1955.
31. Huennekens, F.M., and S.P. Felton, in S.P. Colowick and N.O. Kaplan, (eds), Methods of Enzymology, Vol. III, Academic Press, New York: 1957, 955.
32. Umbreit, W.W., R.H. Burris, and J.F. Stauffer, Manometric Techniques, Burgess Publishing Co., Minneapolis: 1964.
33. Bergmeyer, H.V., (ed), Methods of Enzymatic Analysis, Academic Press, New York: 1963, 124.
34. Hugget, A. St.G. and D.A. Nixon, Lancet, 2:368 (1957).
35. Hugget, A. St.G. and D.A. Nixon, Biochem. Journal, 66:12 (1957).
36. Kondo, H., H.C. Friedman, and B. Vennesland, J. Biol. Chem. 234: 1533 (1960).

37. Stahl, E., Thin Layer Chromatography, Springer-Verlag, New York: 1965.
38. Knight, Jr., E. and R.W.F. Hardy, J. Biol. Chem. 241:2752 (1966).
39. Hinkson, J.W., and W.A. Bulen, J. Biol. Chem. 242:3345 (1967).
40. Massey, V., G. Palmer, C.H. Williams Jr., B.E.P. Swoboda, and R.H. Sands in E.C. Slater, (ed), Flavins and Flavoproteins, Elsevier Publishing Co., London: 1966, 133.
41. Massey V., and G. Palmer, Biochem. 5:3181 (1966).
42. Dixon, M., and E.C. Webb, Enzymes, Academic Press, New York: 1964, 443ff, 117.
43. Friedwald, J.S., and G.D. Maengwyn-Davies in W.D. McElroy and B. Glass, (eds), The Mechanism of Enzyme Action, Johns Hopkins Press, Maryland: 1954, 157.
44. Webb, J.L., Enzyme and Metabolic Inhibitors, Vol. I, Academic Press, New York: 1963, 55ff, 151, 552ff.
45. Whittenberger, C.L., and A.S. Haaf, Biochemica et Biophys. Acta, 122:393 (1966).
46. Massey, V., Biochem. J., 53:67 (1953).
47. Webb, E.C., and P.F.W. Morrow, Biochem. J., 73:7 (1959).
48. Fridovich, I., and P. Handler, J. Biol. Chem., 228:67 (1957).
49. Fridovich, I., and P. Handler, J. Biol. Chem., 231:899 (1958).
50. Fridovich, I., and P. Handler, J. Biol. Chem., 233:1581 (1958).
51. Fridovich, I., and P. Handler, J. Biol. Chem., 236:1836 (1961).
52. Handler, P., K.V. Rajagopalan, and V. Aleman, Fed. Proc., 23:30 (1964).
53. Massey, V., J. Biol. Chem., 229:763 (1957).
54. Fridovich, I., and P. Handler, J. Biol. Chem., 237:916 (1962).
55. Miller, R.W., and V. Massey, J. Biol. Chem., 240:1466 (1965).

APPENDIX

DERIVATION OF THE RELATIONS USED IN DETERMINING THE K_m FOR DIHYDROOROTATE AND A METHOD FOR DETERMINING K_i FOR OROTATE

The following derivation is based upon equilibrium kinetics where it is assumed that an inhibitor can either affect the affinity of the enzyme for its substrate or change the rate at which the enzyme-substrate complex breaks down into enzyme and products (44, p.56). Such a relationship is shown in equation 1:



Where: E = enzyme, S = substrate, P = product, I = inhibitor, ES = enzyme-substrate complex, EI = enzyme-inhibitor complex, EIS = enzyme-inhibitor-substrate complex,

and: α = change in the affinity caused by the inhibitor

β = inhibitor induced change in the rate of complex decomposition.

$$K_s = \text{dissociation constant of the ES complex} = \frac{(E)(S)}{(ES)} \quad (\text{Eq. 2})$$

(analogous to K_m)

$$K_i = \text{dissociation constant of the EI complex} = \frac{(E)(I)}{(EI)} \quad (\text{Eq. 3})$$

$$\alpha K_s = \text{dissociation constant of the EIS complex} = \frac{(EI)(S)}{(EIS)} \quad (\text{Eq. 4})$$

$$\gamma K_i = \text{dissociation constant of the EIS complex} = \frac{(ES)(I)}{(EIS)} \quad (\text{Eq. 5})$$

During an inhibited enzymatic reaction the total enzyme concentration is represented by Equation 6:

$$(E_t) = (E) + (ES) + (EI) + (EIS) \quad (\text{Eq. 6})$$

and the rate of product formation by Equation 7:

$$\left(\frac{dp}{dt} \right)_i = V_i = k(ES) + \beta k(EIS) \quad (\text{Eq. 7})$$

So that Equation 6 may be expressed entirely in terms of the ES complex, Equations 2 to 5 are rearranged and substituted as follows:

$$K_s = \frac{(E)(S)}{(ES)} \longrightarrow (E) = (ES) \frac{K_s}{(S)} \quad (\text{Eq. 8})$$

$$K_i = \frac{(E)(I)}{(EI)} \longrightarrow (EI) = \frac{(E)(I)}{K_i} = \frac{K_s}{K_i} \frac{(ES)(I)}{(S)} = (ES) \frac{(I)(K_s)}{(S) K_i} \quad (\text{Eq. 9})$$

$$\alpha K_s = \frac{(EI)(S)}{(EIS)} \longrightarrow (EIS) = \frac{(EI)(S)}{\alpha K_s} = \frac{(ES)(I)K_s}{(\cancel{S})K_i} \frac{(\cancel{S})}{\alpha K_s} = (ES) \frac{(I)}{\alpha K_i} \quad (\text{Eq. 10})$$

$$\gamma K_i = \frac{(ES)(I)}{(EIS)} \longrightarrow (EIS) = \frac{(ES)(I)}{\gamma K_i} = (ES) \frac{(I)}{\gamma K_i}$$

The constants α and γ are found to be equal by Equating equations 10 and 11:

$$(ES) \frac{(I)}{\alpha K_i} = (ES) \frac{(I)}{\gamma K_i} \quad \therefore \alpha = \gamma$$

$$\text{Summarizing:} \quad (E) = (ES) \frac{K_s}{(S)} \quad (\text{Eq. 8})$$

$$(EI) = (ES) \frac{(I)(K_s)}{(S)(K_i)} \quad (\text{Eq. 9})$$

$$(EIS) = (ES) \frac{(I)}{\alpha K_i} \quad (\text{Eq. 12})$$

Substituting Equation 8, 9, and 12 into Equation 6 yields:

$$E_t = (ES) \left[\frac{K_s}{(S)} + 1 + \frac{(I)(K_s)}{(S)(K_i)} + \frac{(I)}{\alpha K_i} \right] \quad (\text{Eq. 13})$$

Rearranging:

$$\begin{aligned} (ES) &= \frac{E_t}{\frac{K_s}{(S)} + 1 + \frac{(I)K_s}{(S)K_i} + \frac{(I)}{\alpha K_i}} \\ &= \frac{E_t \alpha (S) K_i}{\alpha K_i K_s + \alpha (S) K_i + \alpha (I) K_s + (S)(I)} \end{aligned} \quad (\text{Eq. 14})$$

Substituting Equation 12 for (ES) by Equation 14:

$$\begin{aligned} (EIS) &= \frac{E_t \alpha (S) K_i (I)}{[\alpha K_i K_s + \alpha (S) K_i + \alpha (I) K_s + (S)(I)] \alpha K_i} \\ &= \frac{E_t (S) (I)}{\alpha [K_i K_s + (S) K_i + (I) K_s] + (S)(I)} \end{aligned} \quad (\text{Eq. 15})$$

Substituting relations 14 and 15 into Equations 7 yields:

$$\begin{aligned} V_i &= k \frac{E_t \alpha (S) K_i}{\alpha [K_i K_s + (S) K_i + (I) K_s] + (S)(I)} \\ &\quad + \beta k \frac{E_t \alpha (S) K_i}{\alpha [K_i K_s + (S) K_i + (I) K_s] + (S)(I)} \\ &= \frac{k(S)(E_t) [\alpha K_i + \beta (I)]}{\alpha [K_i K_s + (S) K_i + (I) K_s] + (S)(I)} \end{aligned} \quad (\text{Eq. 16})$$

If an uninhibited enzyme reaction is allowed to proceed at saturating substrate concentrations then essentially all of the enzyme is in the form of the enzyme-substrate complex. Under these conditions $V_i = k(ES)$ may be written as $V_{max} = k(E_t)$, where V_{max} is the reaction rate at saturating substrate concentrations. Applying this assumption to Equation 16 yields the general rate equation:

$$V_i = \frac{V_{max} (S) [\alpha K_i + \beta (I)]}{\alpha [K_i K_s + (S) K_i + (I) K_s] + (S)(I)} \quad (\text{Eq. 17})$$

Equation 17 may be written in the Michaelis form:

$$V_i = \frac{(S) \left[\frac{V_{max} \alpha K_i + \beta (I)}{\alpha K_i + (I)} \right]}{(S) + K_s \left[\frac{\alpha K_i + \alpha (I)}{\alpha K_i + (I)} \right]} = \frac{(S) V_{max}'}{(S) + K_m'}$$

where the observed maximum velocity, $V_{max}' = V_{max} \frac{\alpha K_i + \beta (I)}{\alpha K_i + (I)}$ (Eq. 18)

and the observed K_m , $K_m' = K_s \frac{\alpha K_i + \alpha (I)}{\alpha K_i + (I)}$ (Eq. 19)

Equation 19 shows how the observed K_m (K_m') of an enzymatic reaction varies with inhibitor concentration. If the inhibitor exhibits completely competitive inhibition, then in relation to Equation 1 and 19 $\alpha = \infty$.

Applying this value of α to Equation 19 (rewritten in Equation 20):

$$K_m' = K_s \frac{\alpha [K_i + (I)]}{\alpha [K_i + 1/\alpha (I)]} \quad (\text{Eq. 20})$$

as $\alpha \rightarrow \infty$, $1/\alpha \rightarrow 0$ and Equation 20 becomes:

$$K_m' = K_s \frac{K_i + (I)}{K_i} = K_s \left(1 + \frac{(I)}{K_i} \right) = K_s \left(\frac{1}{K_i} (I) + 1 \right) \quad (\text{Eq. 21})$$

It can be seen from Equation 21 that if one plots K_m' vs (I) a straight line will result from which K_s may be obtained from the ordinate intercept at $(I) = 0$ and K_i may be determined from the slope.